

NASA Contractor Report 4315

Structure-Borne Noise Estimates for the PTA Aircraft

James F. Unruh

CONTRACT NAS1-17921
AUGUST 1990

(NASA-CR-4315) STRUCTURE-BORNE NOISE
ESTIMATES FOR THE PTA AIRCRAFT (Southwest
Research Inst.) 61 p CSCL 20A

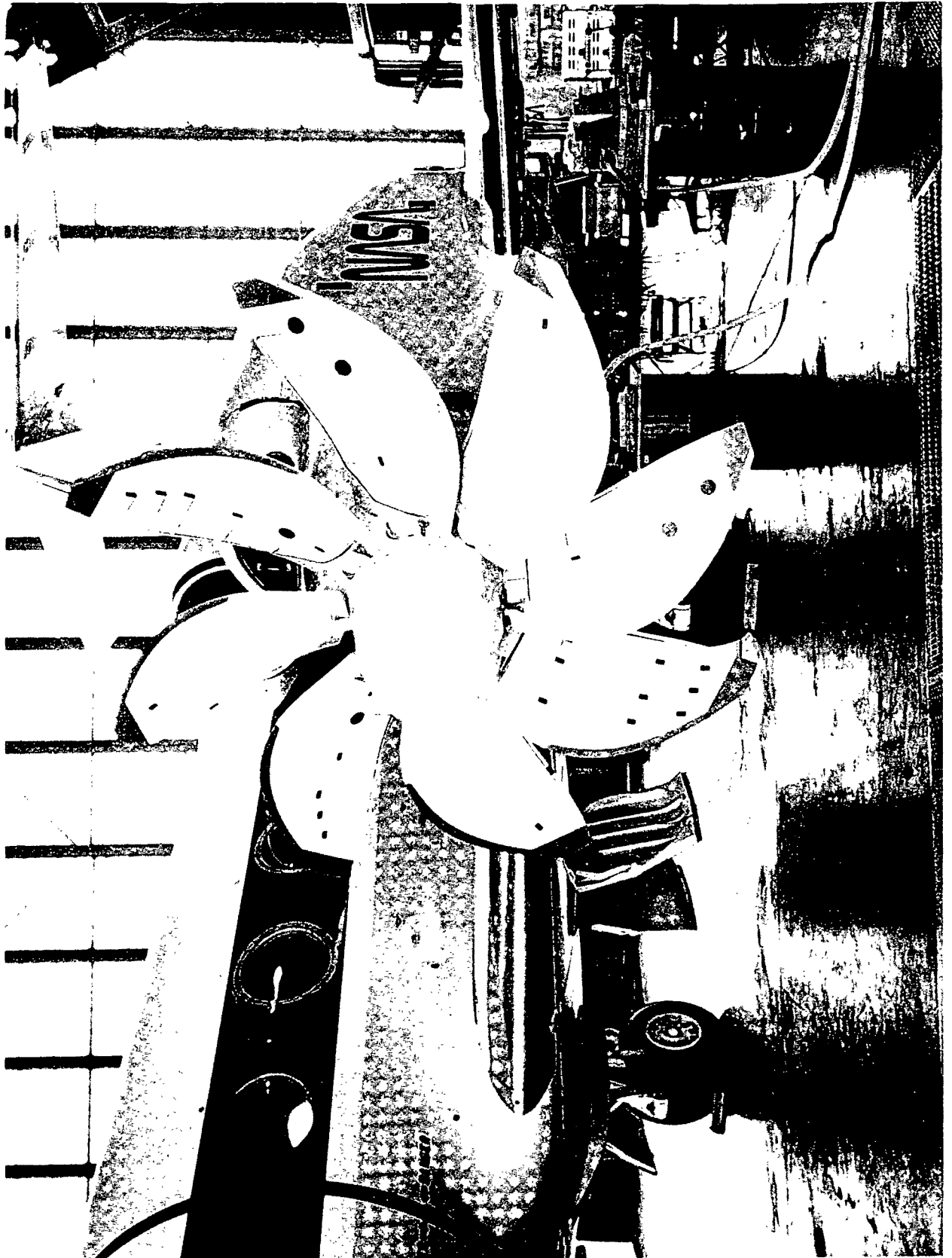
N90-28396

Unclass
H1/71 0293198

NASA

Structure-Borne Noise Estimates for the PTA Aircraft

ORIGINAL PAGE
BLACK AND WHITE PHOTOGRAPH



NASA Contractor Report 4315

Structure-Borne Noise Estimates for the PTA Aircraft

James F. Unruh
Southwest Research Institute
San Antonio, Texas

Prepared for
Langley Research Center
under Contract NAS1-17921



National Aeronautics and
Space Administration
Office of Management
Scientific and Technical
Information Division

1990

TABLE OF CONTENTS

	<u>Page</u>
List of Tables.....	vii
List of Figures.....	viii
Nomenclature.....	x
I. INTRODUCTION.....	1
II. IN-FLIGHT STRUCTURE-BORNE NOISE DETECTION TECHNIQUE...	3
A. Test Procedure.....	3
III. PTA FLIGHT TEST DATA.....	5
A. Cabin Microphone Locations.....	5
B. Wing Strain Gage Locations.....	5
C. Test Conditions.....	5
D. Typical Response Data.....	6
IV. PTA GROUND TEST.....	7
A. Test Setup - Shaker Excitation.....	7
B. Instrumentation.....	7
1.0 Interior Microphones.....	7
2.0 Wing Root Strain Gages.....	8
3.0 Force Cells.....	8
C. Signal Conditioning and Control.....	8
D. Data Acquisition.....	9
E. Data Reduction.....	10
F. Typical Test Results.....	10
1.0 Wing Excitation.....	10
2.0 Strain Gage and Microphone Signals.....	11
3.0 Frequency Response Functions.....	11
V. ESTIMATES OF IN-FLIGHT STRUCTURE-BORNE NOISE.....	13
A. Flight Conditions.....	13
B. Estimation Procedures.....	13
C. Results.....	13
1.0 Flight Parameter Effects.....	14
D. Discussions.....	14

VI.	CONCLUSIONS AND RECOMMENDATIONS	17
VII.	REFERENCES	19

LIST OF TABLES

<u>Table No.</u>		<u>Page</u>
1	Cabin Microphones Internal - Fixed.....	21
2	Left Hand Wing Strain Gage Locations.....	22
3	Typical PTA In-Flight Data File.....	23 thru 25
4	List of Signal Conditioning and Recording Equipment.....	26
5	Data Acquisition Schedule.....	27
6	PTA In-Flight Structure-Borne Noise Estimates, First Blade Passage Tone	28 thru 29
7	PTA In-Flight Structure-Borne Noise Estimates, Second Blade Passage Tone	30 thru 31
8	PTA In-Flight Structure-Borne Noise Estimates, Third Blade Passage Tone	32 thru 33

LIST OF FIGURES

<u>Figure No.</u>		<u>Page</u>
1	PTA Testbed Aircraft.....	35
2	In-Flight Structure-Borne Noise Detection Concept.....	36
3	Cabin Microphone Locations.....	37
4	Typical In-Flight Fixed Microphone Installation.....	38
5	Shaker and Strain Gage Locations.....	39
6	Photographs of Test Set-Up.....	40 thru 41
7	FRF Ratio of Shaker Excitation F_{INBD}/F_{OUTBD}	42
8	Typical Background Noise Levels.....	43
9	Typical Recorded Signal Levels.....	44
10	Interior SPL Response to Unit Micro Strain at SG05A.....	45
11a	PTA In-Flight SBN Versus Engine/Propeller Power, First Blade Passage Tone.....	46
11b	PTA In-Flight SBN Versus Engine/Propeller Power, Second Blade Passage Tone.....	47
11c	PTA In-Flight SBN Versus Engine/Propeller Power, Third Blade Passage Tone.....	48
12a	PTA In-Flight SBN Versus Flight Altitude, First Blade Passage Tone.....	49
12b	PTA In-Flight SBN Versus Flight Altitude, Second Blade Passage Tone.....	50
12c	PTA In-Flight SBN Versus Flight Altitude, Third Blade Passage Tone.....	51
13a	PTA In-Flight SBN Versus Mach Number, First Blade Passage Tone.....	52
13b	PTA In-Flight SBN Versus Mach Number, Second Blade Passage Tone.....	53

13c	PTA In-Flight SBN Versus Mach Number, Third Blade Passage Tone.....	54
14	Difference of In-Flight and Structure-Borne Noise Levels Versus Frequency	55

NOMENCLATURE

$HPM(\omega)_j$	moment to interior pressure frequency response function
$HXM(\omega)_j$	moment to structural response frequency response function
$HPX(\omega)_{jk}$	structural response to interior pressure frequency response function
$P(\omega)_j$	pressure response at the j^{th} microphone
$\bar{P}(\omega)_j$	computed pressure response at the j^{th} microphone
$M(\omega)$	input moment
$X(\omega)_k$	structural response at the k^{th} location
$\bar{X}(\omega)_k$	in-flight measured structural response at the k^{th} location

I. INTRODUCTION

Under a contract from NASA Lewis Research the Lockheed-Georgia Company modified a Gulfstream GII business jet transport to evaluate the application of an advanced turboprop propulsion system on a transport aircraft. The primary aircraft modification was the addition of a Hamilton Standard/NASA SR-71 propfan and Allison Model 501-M78 6,000 horsepower drive system to the left wing of the 66,500 pound maximum takeoff gross weight aircraft. The modified Gulfstream was called the Propfan Test Assessment (PTA) aircraft. The various aircraft modifications are shown schematically in Figure 1, as taken from Reference 1. The PTA program objective was to evaluate the propfan structural integrity, propfan source noise, and propfan cabin noise and vibration.

The PTA aircraft underwent flight test evaluation during the March 1987 to March 1988 time period. Results from the flight test were documented and presented to the aircraft community as a PTA Flight Test Results Review at NASA Lewis Research Center on November 14, 1988. One of the primary concerns of the propfan configuration is the cabin noise environment. The PTA flight test aircraft consisted of a pressurized bare cabin with noise levels dominated by blade-order tones of maximum level 120 dB with a 15 to 20 dB variation within the cabin. It was concluded that a side wall treatment with a target insertion loss near 40 dB would be required to reduce the interior noise levels to an overall of about 80 dBA (ref. 1).

Ground tests were also conducted to detect structure-borne noise transmission into the PTA cabin via application of discrete and random forces to the wing front and rear spars, using an electromagnetic shaker. From correlation of the generated cabin noise and wing accelerations with in-flight wing vibration levels it was concluded that structure-borne noise transmission levels due to combined propeller wake/vortex impingement on the wing surface and engine/gear box vibration was not evident, but in certain circumstances, it could be plausible (ref. 1).

The investigation reported herein is an independent evaluation of the in-flight structure-borne noise transmission levels in the PTA test aircraft based on the in-flight measured wing front and rear spar dynamic strain levels. The structure-borne noise detection technique employed was previously developed under laboratory simulation (ref. 2) and is briefly described in Section II. The data available from the PTA flight test which was used during the investigation will be discussed in Section III. The required ground tests of the PTA aircraft are discussed in Section IV with estimates on the level of structure-borne noise transmission given in Section V.

Use of trade names or names of manufacturers in this report does not constitute an official endorsement of such products or manufacturers, either expressed or implied, by the National Aeronautics and Space Administration.

II. IN-FLIGHT STRUCTURE-BORNE NOISE DETECTION TECHNIQUE

The laboratory based development of a procedure for the detection of structure-borne noise transmission in an aircraft due to propeller wake/vortex impingement on the wing structure or due to engine/propeller vibration is reported in References 2 and 3. This procedure was employed for the present study and will be discussed briefly in the following paragraphs.

A. Test Procedure

The test procedure for detection of in-flight propeller-induced structure-borne noise is most easily described with reference to the schematic of Figure 2. The structural path, being the wing structure, is excited with a dynamic moment M in the area of the propeller wake and NS structural response measurements X_k are acquired, along with NP interior microphone responses P_j . During ground test measurements, the pressure response to input moment,

$$HPM(\omega)_j = P(\omega)_j / M(\omega)$$

frequency response functions (FRF's) are computed along with structural response to input force FRF's.

$$HXM(\omega)_k = X(\omega)_k / M(\omega)$$

The pressure response to structural excitation FRF's are then computed as

$$HPX(\omega)_{jk} = HPM(\omega)_j / HXM(\omega)_k.$$

During flight test, the structural responses $\bar{X}(\omega)_k$ are acquired and estimates of interior structure-borne noise levels $\bar{P}(\omega)_{jk}$ are computed for the ground-based FRF's as

$$\bar{P}(\omega)_{jk} = HPX(\omega)_{jk} * \bar{X}(\omega)_k$$

A variation in computed interior levels occurs from use of multiple structural response measurements and multiple microphone response locations within the receiving cabin.

In the original development of the above procedure various methods of wing excitation were evaluated including hammer impact at discrete wing locations, single shaker discrete frequency excitation and dual shaker sweep excitation (ref 3). However, it was found that for propeller wake/vortex simulation the use of dual shakers, driven 180 degrees out of phase, provided the proper excitation, a pure dynamic moment about the propeller axis (ref 4). It was

also found that wing spar strain was a more reliable structural response parameter than wing or cabin acceleration response. The application of this procedure to the PTA aircraft is discussed in Section IV.

III. PTA FLIGHT TEST DATA

The PTA testbed aircraft was equipped with a variety of acoustic, vibration, and propeller and aircraft performance monitoring instrumentation wired into an on-board data acquisition system for in-flight collection of the various parameter responses. Reference 1 describes in detail the numbers and locations of the instrumentation, herein only those transducers of direct interest to the present effort will be described.

A. Cabin Microphone Locations

A total of 37 interior cabin microphones were used during the PTA flight test. Only the 18 fixed position wall mounted microphone locations were used during the present effort. The remaining microphones were mounted to a microphone tram assembly which could be traversed along the length of the fuselage. The tram assembly was not installed during the ground tests and therefore the additional microphone locations were not readily available. The fixed wall mounted microphone locations were obtained from Lockheed engineers and are listed in Table 1. A schematic of the microphone locations is given in Figure 3 and a photograph of typical microphone in-flight installation is given in Figure 4. As will be discussed in Section IV, the microphones used during the flight test were not available for use during the present ground test evaluation.

B. Wing Strain Gage Locations

The PTA testbed aircraft wing was heavily instrumented with 44 microphones, 33 accelerometers, and 14 strain gages. The only strain gages used on the aircraft were mounted on the wing front and rear spars, an ideal location for the present study (ref. 2). A list of the 14 gages and their respective wing locations is given in Table 2 and a general schematic of their locations is given in Figure 5. The strain gages denoted with an A, such as SG01A versus SG01, were mounted 3/4 inch from the primary gage. The strain gages were Micro-Measurement CEA-13-062 UW/350 type with a gage factor of 2.15.

C. Test Conditions

The test matrix covers a range of flight altitudes from 5,000 to 40,000 feet, flight Mach Numbers ranging from 0.28 to 0.85, and propeller power ranging from approximately 560 to 5,950 shaft horsepower. The resulting fundamental blade passage frequency varied from 173.7 to 236.8 Hz. The effect of nacelle tilt angle was also evaluated with test data acquired at nacelle tilt angles of -1, -3, and +2 degrees. Data were acquired for a total of 549 test points. The present evaluation was limited to the primary nacelle tilt angle of -1 degrees as is discussed below.

D. Typical Response Data

The data made available for the present evaluation were in the form of peak microphone and strain responses at the fundamental blade passage frequency and its first 9 harmonics. Only responses at the first three propeller tones were of interest in the present study due mainly to limited strain response data above the background noise at frequencies above 800 Hz. The primary flight test data file was delivered on a VAX TK50-K CompacTape in VMS backup format. The data file occupied approximately 80,000 blocks of disk space. The binary data file was delivered with a NASA generated FORTRAN source code which, with straight forward modification, enabled reading select flight data retrievable via a unique Condition Number corresponding to a desired Flight Number and Run Number. A typical data file is shown in Table 3. This data is from Flight 23 - Run 17 which corresponds to Condition Number 710. The microphone response level is given in dB reference 2×10^{-5} Pascals and, as can be seen, no response was recorded on microphone MC03 which is typical throughout the data bank. Strain signal levels are given in micro strain and a level of -1 indicates no peak or tone level above the background. Typically strain responses at propeller tone 3 were limited to only a few gages or none at all.

Unfortunately, several of the peak strain signals extracted from the raw data tapes and placed in the PTA data bank were found to contain a voltage to engineering units scale factor error. The error was a factor of 1000 which arose from working with volts rather than millivolts. The data bank errors were generally not present throughout a given Flight Condition and as such were quite apparent upon detailed visual inspection of the strain data. By working directly with Lockheed engineers, it is believed that all such errors have been corrected for the data presented in this report. To the authors knowledge, the original PTA data bank strain levels have not been corrected.

IV. PTA GROUND TEST

Ground based tests on the Propfan Test Assessment (PTA) aircraft stationed at NASA Lewis Research Center were carried out during the week of June 5, 1989. The objective of the ground tests was to acquire frequency response functions (FRF) of interior microphone to wing strain response for the purpose of estimating the level of interior structure-borne noise (SBN) transmission during aircraft flight. The test setup, instrumentation, signal conditioning and control equipment, data acquisition and data reduction will be discussed briefly in the following paragraphs.

A. Test Setup - Shaker Excitation

The general arrangement of the test apparatus is shown in Figure 6a. Two Unholtz Dickie Model #1 50 lb modal, current driven, shakers were attached to the PTA lower wing hard structure. The shakers were driven harmonically, in the frequency range from 150 Hz to 750 Hz, 180 degrees out-of-phase to produce a pure dynamic moment excitation simulating the propeller wake excitation. With shaker cooling air, supplied to the shakers by the blower and hose arrangement shown in the foreground of Figure 6a, the maximum output force of either shaker was 30 lb. The shakers were originally attached to the wing ribs symmetric about the engine nacelle at BL 140.0 and BL 192.0, as indicated in Figure 5. However, it was found that constant force control at the outboard shaker location (BL 192.0) could not be achieved which required movement of the shaker to the next outboard rib at BL 210.0. The 70 inch shaker spacing resulted in a maximum excitation of 2100 in-lb (175 ft-lb) dynamic moment. The frequency range of excitation covers the first three propeller tones for the various propeller speeds encountered during the PTA flight tests.

B. Instrumentation

1.0 Interior Microphones

Interior noise level measurements at the 18 fixed microphone locations used during the PTA flight tests were recorded during the shaker induced wing excitations. The microphone locations are listed in Table 1 and are shown schematically in Figure 3, as taken from Reference 1. Flight test photographs of microphone installations were available to help locate the 18 fixed microphone locations. Several errors in the listed Water Line locations were discovered and corrections were made as noted in Table 1 under "SwRI". The data at the 18 locations were acquired with three microphones during six independent data runs. Typical microphone installation is shown in the photograph of Figure 6c. Bruel & Kjaer 1/2 inch Type 4166

microphones and Type 2615 preamplifiers were used to acquire the cabin acoustic response. A Bruel & Kjaer Type 4230 sound level calibrator supplying a 94 dB (ref. 2×10^{-5} Pascals) sound pressure level at 1 kHz provided calibration of the microphones. Cables from the microphone preamplifiers were routed to the aircraft exterior via a floor level cable race to the landing gear wheel well.

2.0 Wing Root Strain Gages

A list of the left hand wing strain gage locations is given in Table 2 and Figure 5 schematically shows several of the gage locations. The strain gages denoted with an A, such as SG01A versus SG01, are 3/4 inch from the primary gage. As such the adjacent gages would provide only redundant data for structure-borne noise (SBN) estimates and therefore only the eight primary gages were of interest during the ground test. However, due to signal problems with gages SG02 and SG05 the adjacent gages SG02A and SG05A were used, respectively. Calibration of the strain gage signals was based on the 2.15 gage factor. Signal lines from the strain gages were intercepted prior to the PTA on-board data acquisition system and routed, via a floor level cable race, to signal conditioning equipment.

3.0 Force Cells

Kistler Instruments Model 9212 force cells were attached between the wing and the modal shakers to regulate and record the excitation force levels, reference Figure 6b. While current supplied to the modal shaker is generally a good indicator of the input load, the force cell provided a much more accurate indication of actual input force due to potential compliance of the shaker to wing attachment rods.

C. Signal Conditioning and Control

The signal conditioning and control equipment used to conduct the SBN ground tests is shown in Figure 6d. A list of the equipment is given in Table 4 along with a functional description. For clarification, Table 4 also shows the equipment schematically located as given in the photograph of Figure 6d.

Shaker control is ideally achieved via routing of the force cell signals to the Endevco 6330 charge amplifiers-(5), with one amplified output each routed to the Spectral Dynamics 105 amplitude servo/monitors-(6&7). The servo/monitors also receive a desired drive signal from the Spectral Dynamics 104 sweep oscillator-(8) and adjust their output to drive the Unholtz Dickie TA35 current amplifiers-(1) to compensate for any deviations in the monitored shaker force cell signals. The shaker current amplifiers are equipped with a front panel switch to achieve

180 degree phase shift. Unfortunately, one of the amplitude servo/monitors was damaged during shipment to NASA and could not maintain amplitude control. Thus, a single amplitude servo/monitor was used to control the outboard shaker while the inboard shaker was driven open loop with the outboard shaker drive signal. As will be seen in the Typical Results Section below, this arrangement resulted in surprisingly good moment excitation control. Such good moment control with a single controller is attributed to the use of a matched pair of shakers and amplifiers and nearly equivalent driving point impedance at the shaker to wing attachments.

Signals for the three cabin mounted microphones were high pass filtered via ITHACO Model 4502 filters-(10) and then amplified for recording with a nominal gain of 20 via HEAD Model 107 instrumentation amplifiers-(12).

The eight channels of wing root strain signals were routed directly to the Measurement Group Model 2120A strain gage conditioner/amplifier-(15) which provided a balancing bridge with a gain of 2100 on all channels. The low frequency (150 to 750 Hz) strain signals were quite weak, nominally less than 1 micro strain, which required additional amplification on the order of 100 supplied by Trig-Tek Model 205B instrumentation amplifiers-(11). Unfortunately, a high frequency signal, of approximately 40 kHz, dominated the strain signals at the high gains required for recording. It is believed that the signal was generated in the hanger from a sonar device used to eliminate bird nesting, unfortunately no one knew how to turn off the device. The required eight channels of low pass filters were not available to remove the high frequency noise, however, single stage RC filters set at 1600 Hz were developed from available components and were used between the strain gage conditioner and Trig-Tek amplifiers thus reducing the unwanted signals to acceptable levels for recording.

D. Data Acquisition

The strain gage, microphone, and load cell signals were recorded on a TEAC XR50 14 channel cassette data recorder-(9) according to the channel assignment schedule given in Table 5. The six data runs allowed for recording interior noise levels at all 18 fixed microphone locations. A logarithmic frequency sweep in the range from 150 to 750 Hz was made at a sweep rate of 0.1 decade per minute. A sweep rate of 0.3 decade per minute was shown to yield equivalent responses and therefore the slower rate was felt to be adequate. Sine wave calibration signals were recorded on the tape prior to data acquisition and a segment of background noise was recorded after completion of the six data runs. Most all data recording was carried out after the normal NASA work day to prevent unwanted background noise.

E. Data Reduction

On site data reduction and signal monitoring was carried out via the ZONIC 6080-(2) for time window and spectral analysis and a Tektronix SC502 oscilloscope-(14) for continuous time signal monitoring. A Compaq 386 personal computer-(3) was used as a control terminal to the ZONIC analyzer. The sweep data were spectrally analyzed in a 1000 Hz data window with 2.5 Hz bandwidth of analysis using a periodic flat-top data window with an effective 23 % data overlap. Under these conditions, the analyzer required approximately 1365 sample averages to complete the logarithmic sweep.

Post data analysis used a similar setup as that used for on-site data reduction, however, permanent digital data records were stored in the Compaq 386 for frequency response functions between all microphone and strain responses (18 microphones by 8 strain gages to yield 144 FRF's). During the data reduction process the low level strain response signals were passed through a narrow band tracking filter driven by the shaker load cell response signal. The narrow band filtering greatly enhanced the strain signal to noise ratio. The microphone signals were of sufficient quality to allow direct analysis and therefore no additional filtering was necessary. Since only the magnitude of the FRF's are of interest in estimating SBN, the phase shifts in the various signal conditioning, recording, and data analysis setups between the various strain and microphone signals were not taken into account in the data reduction process.

F. Typical Test Results

1.0 Wing Excitation

The frequency response function (FRF) between the force excitation at the inboard shaker to that of the outboard shaker, controlled to a constant 30 lb amplitude, should yield a quantitative measure of success in producing a pure dynamic moment excitation. The data of Figure 7 gives the desired FRF where in it can be seen that shakers remained 180 degrees out of phase well above 700 Hz, and only after 700 Hz did the force ratio vary more than approximately 20 percent. It is of interest to note that the highest blade passage frequency (BPF) of interest for SBN estimates for the PTA tests was 237.5 Hz. This translates to 712.5 Hz for the third BPF as indicated by the dashed line in Figure 7. Only small deviations from the desired pure dynamic moment excitation existed in the frequency range of interest to this study. Due to an oversight during recording, the inboard shaker force level between 150 to 200 Hz was over written with the tape voice log. The operator was under the belief that the voice log was on the unused channel 14.

The shaker force levels are of no direct interest other than for the above evaluation and for providing a frequency source for the strain signal tracking filter which was obtained directly from the outboard shaker force cell signal.

2.0 Strain Gage and Microphone Signals

Typical signal background noise levels recorded during the ground test are given in Figure 8. The background strain level shown for SG05A in Figure 8 exhibits a nominal amplitude of 0.03 micro-strain in the 150 to 750 Hz frequency range. The PTA interior background noise levels for microphones MC09, MA05, and MA06 are nominally below 50 dB.

The signal power spectra normally computed during sample averaging of a logarithmic sweep do not reflect the peak values used to obtain the desired FRF signal ratios. Since we are interested in the signal levels while the excitation is applied, a ZONIC 6088 analyzer was employed to capture the peak signal levels during the sample averaging process. Typical signal spectral levels for strain gage SG05A and microphones MC09, MA05, and MA06 are given in Figure 9. As can be seen by comparison to the data of Figure 5, the recorded microphone signals are well above the recorded background noise levels with a 30 to 40 dB margin. The SG05A strain signal level varies from 0.14 to 1.0 micro-strain corresponding to a signal amplitude to noise ratio in the range of approximately 5 to 33, or 13 to 30 dB. It is felt that while the recorded strain levels were very low, the signals were sufficiently strong to establish the necessary FRF data base required for in-flight structure-borne noise transmission estimates for the PTA aircraft. It is of interest to note that the ground test strain levels recorded were on the same order as those measured during the PTA flight test (reference Table 3).

3.0 Frequency Response Functions

Typical strain to interior sound pressure level (SPL) frequency response functions are given in Figure 10 wherein the SPL at microphones MC09, MA05, and MA06 are given for a unit microstrain at SG05A. In general it appears that an 80 to 100 dB interior sound pressure level will result from a unit wing microstrain. The FRF's of Figure 10 are quite rich in what appears to be resonant response of both the wing structure and the coupled fuselage/cabin structural acoustic environment.

V. ESTIMATES OF IN-FLIGHT STRUCTURE-BORNE NOISE

A. Flight Conditions

Some 50 PTA testbed Flight Conditions were initially evaluated with 40 resulting in apparently valid data. A variety of flight altitudes, Mach numbers, and engine/propeller horsepower settings were evaluated. While nacelle tilt angles of -3, -1, and 2 degrees were evaluated during the flight test; generally very poor data, either due to interior microphone dropout or erratic strain level data, were found for the -3 and 2 degree cases. The present study was therefore confined to the -1 degree nacelle tilt configuration which was the primary PTA test configuration.

B. Estimation Procedures

The strain to interior noise frequency response function data obtained during ground test of the PTA aircraft allowed prediction of in-flight structure-borne noise levels at the 18 microphone locations for in-flight measured responses from each of the 8 wing mounted strain gages. Thus, there exists a possibility of 8 noise level estimates at each microphone and a possibility of 144 noise level estimates for the overall cabin response. The in-flight strain level data bank used in this study consisted of peak strain levels at each of the first three propeller tones. In-flight strain levels beyond the third propeller tone were generally not above the background noise. If no identifiable peak occurred in the strain spectrum in the area of the propeller tone, the strain response was set to -1.0 and no contribution to the analysis was taken from that response. The aircraft a.c. power fundamental was a 400 Hz signal which masked the strain response corresponding to the second propeller tone for a number of Flight Conditions. For these cases the strain responses were also set to zero to eliminate their influence on overall noise estimates (this was manually carried out upon review of the in-flight data bank). The interior microphone at location MC03 was inoperative for all in-flight configurations evaluated, however, estimates of structure-borne noise transmission were made for all 18 microphone locations.

C. Results

Energy average overall cabin structure-borne and in-flight noise level estimates were made by equally weighting all responding microphone locations. The results of the analysis for the first three propeller tones (denoted as P1, P2, and P3) are given in Tables 6 through 8, respectively. As can be seen in the tables, estimates for overall cabin noise levels plus one standard deviation are given under the column denoted as +SIG. Also given are the number of

valid estimates used in obtaining the energy averages, denoted as N in the tables. These data are given for the estimated overall structure-borne noise levels and the recorded in-flight levels during the PTA flight test. The maximum, minimum, and average cabin noise levels and noise level plus one standard deviation are also given in the tables, along with the standard deviation (listed as STD. DEV.) of the primary quantities. Likewise, the difference in recorded in-flight cabin overall noise level and estimated structure-borne noise level is given in the last column in the tables.

1.0 Flight Parameter Effects

The estimated structure-borne and recorded in-flight cabin levels of Tables 6 through 8 are presented graphically versus engine/propeller power in Figures 11a, 11b, and 11c, respectively. In general, the estimated structure-borne noise levels are consistent with one standard deviation being approximately 3 dB, and show little correlation with engine/propeller power. Similar conclusions can be drawn for the recorded in-flight noise levels which are also plotted in Figures 11a through 11c.

Similar data are plotted in Figures 12a through 12c for the variation of estimated structure-borne noise transmission versus aircraft flight altitude. Flight altitude appears to be a stronger parameter for the second blade passage tone with decreasing SBN transmission with increasing altitude. However SBN transmission at the first and third blade passage tones appear to be somewhat independent of flight altitude. The variation of SBN transmission with flight Mach number shows similar trends as those with flight altitude, as can be seen in Figures 13a through 13c. One should expect the higher SBN transmission levels at the higher propeller power settings which normally occur at the low altitude and low Mach number Flight Conditions.

D. Discussions

Based on the data presented, it does not appear that the PTA aircraft has a propeller induced structure-borne noise transmission problem. However, the test aircraft was not fitted with a high loss sidewall transmission interior trim sufficient to reduce the airborne noise level to an acceptable 80 dB(A), in fact, the cabin was bare. The effect of a 40 dB insertion loss interior trim on the structure-borne noise transmission is not known; however, one should not expect a one-to-one noise reduction since the basic transmission paths for airborne and structure-borne noise are quite different.

It is to be noted that the difference between recorded in-flight noise levels and the estimated structure-borne noise levels decrease with increasing propeller tone (increasing frequency). This can be seen by the difference values plotted in Figure 14. This trend is mainly due to a general decrease in recorded in-flight noise levels, since the average SBN transmission level remains relative constant with increasing frequency, as can be seen from the average values given in Tables 6 through 8. It is clearly seen in Figure 14 that the standard deviation of the difference in in-flight and structure-borne noise levels markedly increases for the higher blade passage tones. This is somewhat due to a significant decrease in the number of estimates available at the higher blade passage tones. Nevertheless, the trend of a decreasing difference in in-flight and structure-borne noise levels with increasing frequency appears to be supported.

With side wall treatments generally increasing in effectiveness at higher frequencies, the possibility of a dominating structure-borne noise problem in the frequency range of the third propeller tone could be realized. At the time of this evaluation no data could be found showing the relative effectiveness of a high insertion loss side wall trim on propeller-induced structure-borne noise transmission and therefor no further evaluation of this potential problem area could be carried out.

VI. CONCLUSIONS AND RECOMMENDATIONS

Estimates of the level of structure-borne noise transmission in the Propfan Test Assessment aircraft were carried out for the first three blade passage frequencies. The procedure used combined the frequency response functions of wing strain to cabin SPL response obtained during ground test with in-flight measured wing strain response data. The following conclusions are drawn from the results of this study:

- 1) The estimated PTA aircraft cabin overall structure-borne noise levels varied from 64 to 84 dB, with average levels on the order of 74 dB.
- 2) In general, the structure-borne noise levels showed little dependence on engine/propeller power, flight altitude, or flight Mach number, with the only exception being the second blade passage tone which showed a slight decrease in level with increasing flight altitude and flight Mach number.
- 3) In general, the bare cabin in-flight noise levels decreased with increasing propeller tone giving rise to a plausible structure-borne noise transmission problem at the higher blade passage tones. Without knowledge of the effects of a high insertion loss side wall treatment on structure-borne noise transmission no quantitative conclusions can be made.

It is highly recommended that full scale data be obtained on the relative effectiveness of a high insertion loss side wall treatment for airborne noise reduction on the reduction of structure-borne noise transmission due to propeller induced or engine induced wing vibrations.

VII. REFERENCES

1. Poland, D.T.; Bartel, J.E.; and Brown, P.C., "PTA Flight Test Overview," AIAA Paper 88-2803, January 1988.
2. Unruh, J.F.: "Detection of In-Flight Propeller-Induced Structure-Borne Interior Noise Transmission," AIAA Journal of Aircraft, Vol. 24, No. 7, July 1987, pp. 441-446.
3. Unruh, J.F.: "Aircraft Propeller Induced Structure-Borne Noise," NASA CR-4255, October 1989.
4. Unruh, J.F.: "Prediction of Aircraft-Propeller-Induced Structure-Borne Interior Noise," AIAA Journal of Aircraft, Vol. 25, No. 8, August 1988, pp. 758-764.

TABLE 1. CABIN MICROPHONES INTERNAL - FIXED

TRANSDUCER	FUSELAGE STATION	WATERLINE		STRINGER NUMBER	DESCRIPTION
		REFERENCE 1	SwRI		
MA01	247	128.2 119	119	9	Axial Array
MA02	274	128.2 119	119	9	Axial Array
MA03	301	128.2 119	119	9	Axial Array
MA04	328	128.2 119	119	9	Axial Array
MA05	355	128.2 119	119	9	Axial Array
MA06	409	128.2 119	119	9	Axial Array
MC01	274	139.9 119	139.9	1	Circumferential Array
MC02	301	139.9	139.9	1	Circumferential Array
MC03	328	139.9	139.9	1	Circumferential Array
MC04	274	131.7	131.7	5	Circumferential Array
MC05	301	131.7	131.7	5	Circumferential Array
MC06	328	131.7	131.7	5	Circumferential Array
MC07	274	94.1	94.1	13	Circumferential Array
MC08	301	94.1	94.1	13	Circumferential Array
MC09	328	94.1	94.1	13	Circumferential Array
MC10	274	75.4	82.4	17	Circumferential Array
MC11	301	75.4	82.4	17	Circumferential Array
MC12	328	75.4	82.4	17	Circumferential Array

TABLE 2. LEFT HAND WING STRAIN GAGE LOCATIONS

TRANSDUCER	FUSELAGE STATION	BUTT LINE	GAGE DIRECTION	DESCRIPTION
SG01	355	54	Parallel to Spars	Upper Spar Cap
SG01A	355	54	Parallel to Spars	Upper Spar Cap
SG02	355	54	Parallel to Spars	Lower Spar Cap
SG02A	355	54	Parallel to Spars	Lower Spar Cap
SG03	363.5	71	Parallel to Spars	Upper Spar Cap
SG04	363.5	71	Parallel to Spars	Lower Spar Cap
SG05	355.6	54	Parallel to Spars	Forward Web
SG05A	355.6	54	Parallel to Spars	Forward Wed
SG06	458.5	54	Parallel to Spars	Upper Spar Cap
SG06A	458.5	54	Parallel to Spars	Upper spar Cap
SG07	458.5	54	Parallel to Spars	Lower Spar Cap
SG07A	458.5	54	Parallel to Spars	Lower Spar Cap
SG08	457.9	54	Parallel to Spars	Rear Web
SG08A	457.9	54	Parallel to Spars	Rear Web

TABLE 3. TYPICAL PTA IN-FLIGHT DATA FILE

710.00			COND
23.000			FLT
17.000			RUN
1	PROPELLER TONE		
122.63	235.00	Hz	MA01M1X
122.71	235.00	Hz	MA02M1X
111.37	235.00	Hz	MA03M1X
109.05	235.00	Hz	MA04M1X
111.46	235.00	Hz	MA05M1X
102.80	235.00	Hz	MA06M1X
119.67	235.00	Hz	MC01M1X
124.38	235.00	Hz	MC02M1X
0.00000E+00	0.00000E+00	Hz	MC03M1X
121.93	235.00	Hz	MC04M1X
125.16	235.00	Hz	MC05M1X
109.81	235.00	Hz	MC06M1X
114.69	235.00	Hz	MC07M1X
120.55	235.00	Hz	MC08M1X
123.30	235.00	Hz	MC09M1X
115.28	235.00	Hz	MC10M1X
113.55	235.00	Hz	MC11M1X
122.12	235.00	Hz	MC12M1X
0.11807	235.00	Hz	SG01M1X
0.41809E-01	235.00	Hz	SG2AM1X
0.54087E-01	235.00	Hz	SG03M1X
0.92723E-01	235.00	Hz	SG04M1X
0.11276	235.00	Hz	SG5AM1X
0.47902E-01	235.00	Hz	SG06M1X
0.10405	235.00	Hz	SG07M1X
0.25235	232.50	Hz	SG08M1X

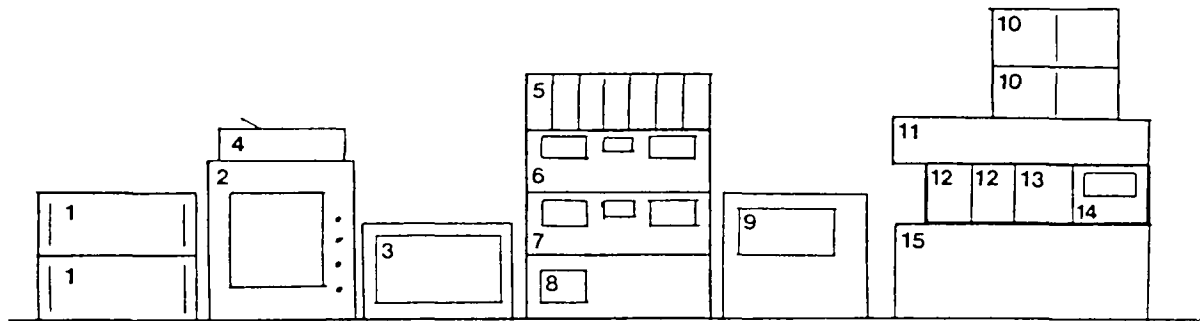
TABLE 3. TYPICAL PTA IN-FLIGHT DATA FILE (Continued)

2	PROPELLER TONE		
109.33	470.00	Hz	MA01M2X
94.670	470.00	Hz	MA02M2X
110.64	470.00	Hz	MA03M2X
112.79	470.00	Hz	MA04M2X
107.41	470.00	Hz	MA05M2X
104.40	470.00	Hz	MA06M2X
110.92	470.00	Hz	MC01M2X
96.760	470.00	Hz	MC02M2X
0.00000E+00	0.00000E+00	Hz	MC03M2X
103.39	470.00	Hz	MC04M2X
111.03	470.00	Hz	MC05M2X
108.45	470.00	Hz	MC06M2X
102.76	470.00	Hz	MC07M2X
98.801	470.00	Hz	MC08M2X
103.94	470.00	Hz	MC09M2X
102.58	470.00	Hz	MC10M2X
109.39	470.00	Hz	MC11M2X
103.33	470.00	Hz	MC12M2X
-1.0000	-1.0000	Hz	SG01M2X
0.66805E-01	470.00	Hz	SG2AM2X
0.49738E-01	470.00	Hz	SG03M2X
0.66041E-01	470.00	Hz	SG04M2X
-1.0000	-1.0000	Hz	SG5AM2X
0.37859E-01	462.50	Hz	SG06M2X
-1.0000	-1.0000	Hz	SG07M2X
0.22785	467.50	Hz	SG08M2X

TABLE 3. TYPICAL PTA IN-FLIGHT DATA FILE (Continued)

3	PROPELLER TONE		
92.718	705.00	Hz	MA01M3X
100.52	705.00	Hz	MA02M3X
90.744	705.00	Hz	MA03M3X
102.23	705.00	Hz	MA04M3X
96.907	705.00	Hz	MA05M3X
94.892	705.00	Hz	MA06M3X
92.544	705.00	Hz	MC01M3X
101.35	705.00	Hz	MC02M3X
0.00000E+00	0.00000E+00	Hz	MC03M3X
90.015	705.00	Hz	MC04M3X
92.731	705.00	Hz	MC05M3X
99.247	705.00	Hz	MC06M3X
99.300	705.00	Hz	MC07M3X
98.872	705.00	Hz	MC08M3X
100.06	705.00	Hz	MC09M3X
94.984	705.00	Hz	MC10M3X
107.21	705.00	Hz	MC11M3X
102.90	705.00	Hz	MC12M3X
-1.0000	-1.0000	Hz	SG01M3X
-1.0000	-1.0000	Hz	SG2AM3X
-1.0000	-1.0000	Hz	SG03M3X
-1.0000	-1.0000	Hz	SG04M3X
-1.0000	-1.0000	Hz	SG5AM3X
0.38342E-01	672.50	Hz	SG06M3X
-1.0000	-1.0000	Hz	SG07M3X
0.10766	702.50	Hz	SG08M3X

TABLE 4. LIST OF SIGNAL CONDITIONING AND RECORDING EQUIPMENT



(Reference Figure 6d)

Item No.	Description	Function
1	Unholtz Dickie TA35/C13628F Current Amplifier	Shaker Excitation
2	Zonic 6080 4 Channel FFT Analyzer	Spectrum Analyzer Data Integrity
3	Compaq 386 Portable PC	Control of Zonic 6080
4	Epson LQ 850 Digital Printer	Hard Copy of Zonic 6080 Output
5	Endevco Model 6330 Charge Amplifier	Excitation for Force Cells
6	Spectral Dynamics 105C Amplitude Servo/Monitor	Control Input to # (1)
7	Spectral Dynamics 105 A Amplitude Servo/Monitor	Control Input to # (1)
8	Spectral Dynamics 104A-5 Sweep Oscillator	Base Signal to # (6) & (7)
9	TEAC XR50 FM 14 Channel Cassette Data Recorder	Data Record
10	ITHACO 450Z Dual 24dB/Octave Filters	High Pass Microphone Signals
11	Trig-Tek Model 205B Instrumentation Amplifier	Strain Gage Signal Amplification
12	Head Precision Model 107 2 Channel Instrumentation Amplifier	Microphone and Strain Gage Signal Amplification
13	Tektronix FG 503 Function Generator	Signal Generator for Calibration
14	Tektronix SC 502 Oscilloscope	Signal Monitor
15	Measurement Group 8 Channel. Strain Gage Conditioner/Amplifier Models 2120A with 2131 Display and 2110 Channel Selector	Strain Gage Conditioning

TABLE 5. DATA ACQUISITION SCHEDULE

Tape Ch 1	Run #1	Run #2	Run #3	Run #4	Run #5	Run #6
1	SG01	--	--	--	--	SG01
2	SG02A	--	--	--	--	SG02A
3	SG03	--	--	--	--	SG03
4	SG04	--	--	--	--	SG04
5	SG05A	--	--	--	--	SG05A
6	SG06	--	--	--	--	SG06
7	SG07	--	--	--	--	SG07
8	SG08	--	--	--	--	SG08
9	MC01	MA01	MC02	MC08	MC03	MC09
10	MC04	MC07	MC05	MC11	MC06	MA05
11	MA02	MC10	MA03	MC12	MA04	MA06
12	F _{OUTBD}	--	--	--	--	F _{OUTBD}
13	FINBD	--	--	--	--	FINBD
14	NOT USED					

**TABLE 6. PTA IN-FLIGHT STRUCTURE-BORNE NOISE ESTIMATES,
FIRST BLADE PASSAGE TONE**

FLT NO.	RUN NO.	NACL TILT	ALT FT	POWER PSHP	MACH NO.	BPF Hz	STRUCTURE-BORNE			IN-FLIGHT			DELTA
							P1	+SIG	N	P1	+SIG	N	P1
15	12	-1	29000	3090	0.7	175	71.5	75.8	144	105.7	109.2	17	34.2
15	13	-1	29000	3187	0.7	182.5	70	74.5	108	107.8	110.5	17	37.8
15	14	-1	29000	3317	0.7	197.5	74.5	78.9	144	112.1	114.8	17	37.6
15	15	-1	29000	3438	0.7	210	72.5	77.4	144	112.3	114.8	17	39.8
15	16	-1	29000	3540	0.7	225	71.8	75.9	126	115	117.9	17	43.2
15	17	-1	29000	3608	0.7	237.5	74	77.7	144	116.2	119.1	17	42.2
16	36	-1	35000	2601	0.8	175	72.5	76.9	108	109.8	112.2	16	37.3
16	37	-1	35000	2624	0.8	175	70.6	74.4	108	109	111.4	16	38.4
16	39	-1	35000	2754	0.8	190	72.3	76.7	108	110.1	113.6	17	37.8
16	41	-1	35000	2874	0.8	205	74.6	78.3	144	112.6	115.1	17	38
16	43	-1	35000	2983	0.8	217.5	73.9	77.8	108	114.2	116.9	17	40.3
16	44	-1	35000	3031	0.8	225	75.6	80	108	115	117.4	17	39.4
16	61	-1	35000	2337	0.8	212.5	72	75.8	144	112.1	114.8	17	40.1
17	16	-1	35000	2601	0.8	175	70.7	74.3	108	108.9	111.5	17	38.2
17	41	-1	35000	3094	0.8	237.5	77.6	82.6	144	118.2	120.3	17	40.6
17	54	-1	40000	2031	0.8	175	71	74.5	108	105.6	108.4	17	34.6
17	55	-1	40000	2194	0.8	197.5	76.2	80.4	108	109.5	112.5	17	33.3
17	56	-1	40000	2358	0.8	225	72.2	76.1	108	111.5	114.5	17	39.3
17	57	-1	40000	2407	0.8	237.5	76.6	81.7	90	115	117.5	17	38.4
18	9	-1	5000	5017	0.28	175	79.3	84.6	90	99.7	102.3	17	20.4
18	12	-1	5000	5219	0.28	190	73.2	78	108	102.4	104.6	17	29.2
18	14	-1	5000	5370	0.28	205	71.8	75.6	126	105.4	107.7	17	33.6
18	15	-1	5000	5441	0.28	210	68.7	72.3	126	107.4	110	17	38.7

**TABLE 6. PTA IN-FLIGHT STRUCTURE-BORNE NOISE ESTIMATES,
FIRST BLADE PASSAGE TONE - (Continued)**

FLT NO.	RUN NO.	NACL TILT	ALT FT	POWER PSHP	MACH NO.	BPF Hz	STRUCTURE-BORNE			IN-FLIGHT			DELTA
							P1	+SIG	N	P1	+SIG	N	P1
18	16	-1	5000	5503	0.28	217.5	66	69.6	90	106.2	108.4	17	40.2
18	24	-1	5000	5915	0.42	225	71	74.3	108	107.5	110.1	17	36.5
19	13	-1	15000	4473	0.35	225	70.4	74.4	108	107.9	111	17	37.5
19	37	-1	15000	3847	0.5	225	73.3	78.4	108	108.5	111.9	17	35.2
19	44	-1	15000	5110	0.6	225	74	78.1	126	116.1	120.1	17	42.1
19	50	-1	15000	5303	0.66	225	72.9	77	126	116.2	120.2	17	43.3
21	13	-1	15000	5303	0.66	225	71	75	126	116.8	120.6	17	45.8
22	45	-1	27000	3595	0.63	225	73.6	77.6	108	113	115.8	17	39.4
22	50	-1	27000	3125	0.47	225	76	79.9	90	106.3	109.4	17	30.3
23	8	-1	27000	3914	0.73	225	75.5	79.9	144	113.3	115.8	17	37.8
23	11	-1	27000	3970	0.83	197.5	80.1	84.6	144	114.6	116.6	17	34.5
23	17	-1	27000	4312	0.83	235	80.9	86.9	144	120.4	123.2	17	39.5
23	19	-1	27000	3625	0.8	175	70.1	73.8	72	109.6	112.2	17	39.5
23	21	-1	27000	4135	0.8	225	72.3	76.9	126	116	118.9	17	43.7
24	28	-1	35000	2773	0.85	175	70.5	74.9	90	110.7	112.8	15	40.2
24	29	-1	35000	2989	0.85	197.5	78.6	83.4	126	114.2	116.5	16	35.6
24	33	-1	35000	3202	0.85	225	76.1	81.8	144	116.2	119	17	40.1

MAXIMUM
MINIMUM
AVERAGE
STD. DEV.

80.9
66
73.39
3.13

86.9
69.6
77.67

120.4
99.7
111.2
4.48

123.2
102.3
114.0

45.8
20.4
37.84
4.39

**TABLE 7. PTA IN-FLIGHT STRUCTURE-BORNE NOISE ESTIMATES,
SECOND BLADE PASSAGE TONE**

FLT NO.	RUN NO.	NACL TILT	ALT FT	POWER PSHP	MACH NO.	BPF Hz	STRUCTURE-BORNE			IN-FLIGHT			DELTA
							P2	+SIG	N	P2	+SIG	N	P2
15	12	-1	29000	3090	0.7	350							
15	13	-1	29000	3187	0.7	367.5	72.3	75.5	36	96.8	99.8	17	24.5
15	14	-1	29000	3317	0.7	395							
15	15	-1	29000	3438	0.7	422.5							
15	16	-1	29000	3540	0.7	452.5	75.8	79.8	108	110.6	113.1	17	34.8
15	17	-1	29000	3608	0.7	472.5	80.7	84.8	108	110.3	112.9	17	29.6
16	36	-1	35000	2601	0.8	350	72.6	76	54	100.4	102.9	16	27.8
16	37	-1	35000	2624	0.8	352.5	70.7	73.5	54	101.4	104.1	17	30.7
16	39	-1	35000	2754	0.8	380	82.5	85.6	36	105	107.9	16	22.5
16	41	-1	35000	2874	0.8	407.5							
16	43	-1	35000	2983	0.8	437.5	78.1	83.2	90	110.7	113.7	17	32.6
16	44	-1	35000	3031	0.8	450	78.1	82.4	108	109.7	112.6	17	31.6
16	61	-1	35000	2337	0.8	422.5							
17	16	-1	35000	2601	0.8	350	68.5	71.4	54	100.7	103.3	17	32.2
17	41	-1	35000	3094	0.8	472.5	80	82.8	90	106	109.7	17	26
17	54	-1	40000	2031	0.8	350							
17	55	-1	40000	2194	0.8	395							
17	56	-1	40000	2358	0.8	452.5	77.9	82.5	90	108.5	111.3	17	30.6
17	57	-1	40000	2407	0.8	472.5	80.5	84.5	108	106.1	109.8	17	25.6
18	9	-1	5000	5017	0.28	350	84.2	87.1	18	88.3	91.5	16	4.1
18	12	-1	5000	5219	0.28	382.5							
18	14	-1	5000	5370	0.28	407.5							
18	15	-1	5000	5441	0.28	422.5							

**TABLE 7. PTA IN-FLIGHT STRUCTURE-BORNE NOISE ESTIMATES,
SECOND BLADE PASSAGE TONE - (Continued)**

FLT NO.	RUN NO.	NACL TILT	ALT FT	POWER PSHP	MACH NO.	BPF Hz	STRUCTURE-BORNE			IN-FLIGHT			DELTA
							P2	+SIG	N	P2	+SIG	N	P2
18	16	-1	5000	5503	0.28	437.5	81.6	86.2	54	90.3	93.2	17	8.7
18	24	-1	5000	5915	0.42	452.5	73.9	78.2	54	99.9	103	17	26
19	13	-1	15000	4473	0.35	450	78.4	83.6	90	98.9	103.6	17	20.5
19	37	-1	15000	3847	0.5	450	78.4	83.3	72	103.6	108.7	17	25.2
19	44	-1	15000	5110	0.6	450	78.6	83.5	108	113	116	17	34.4
19	50	-1	15000	5303	0.66	450	78	82.8	72	113.6	116.2	17	35.6
21	13	-1	15000	5303	0.66	450	77.5	82.5	90	115	117.6	17	37.5
22	45	-1	27000	3595	0.63	450	77.3	81.8	108	109.8	111.5	17	32.5
22	50	-1	27000	3125	0.47	450	79.9	84.6	90	101.4	104	17	21.5
23	8	-1	27000	3914	0.73	450	81.1	86.1	108	108.6	110.7	17	27.5
23	11	-1	27000	3970	0.83	395							
23	17	-1	27000	4312	0.83	470	82	85.9	90	107.7	110.5	17	25.7
23	19	-1	27000	3625	0.8	347.5	72.2	76.3	108	98.8	101.5	16	26.6
23	21	-1	27000	4135	0.8	450	79.4	84.4	144	108	111.2	17	28.6
24	28	-1	35000	2773	0.85	347.5	73.4	77.8	72	101.2	103.7	16	27.8
24	33	-1	35000	3202	0.85	450	83.1	88.9	126	105.8	109.7	16	22.7

MAXIMUM
MINIMUM
AVERAGE
STD. DEV.

84.2
68.5
77.74
3.91

88.9
71.4
81.96

115
88.3
104.6
6.44

117.6
91.5
107.6

37.5
4.1
26.91
7.15

**TABLE 8. PTA IN-FLIGHT STRUCTURE-BORNE NOISE ESTIMATES,
THIRD BLADE PASSAGE TONE**

FLT NO.	RUN NO.	NACL TILT	ALT FT	POWER PSHP	MACH NO.	BPF Hz	STRUCTURE-BORNE			IN-FLIGHT			DELTA
							P3	+SIG	N	P3	+SIG	N	P3
15	12	-1	29000	3090	0.7	527.5	77.9	82.88	36	89.8	92.4	16	11.9
15	13	-1	29000	3187	0.7	550	80.9	84.6	18	93.8	96.9	16	12.9
15	14	-1	29000	3317	0.7	592.5	68	70.3	18	103.9	106.7	17	35.9
15	15	-1	29000	3438	0.7	635	76.1	80.3	54	101.4	104.6	17	25.3
15	16	-1	29000	3540	0.7	677.5	75.6	79.4	90	106.7	109.6	17	31.1
15	17	-1	29000	3608	0.7	710	67.6	72.9	36	112.2	116.2	17	44.6
16	36	-1	35000	2601	0.8	527.5	77.4	82.3	36	98.3	101.7	16	20.9
16	37	-1	35000	2624	0.8	527.5	76	80.8	36	97.5	100.9	17	21.5
16	39	-1	35000	2754	0.8	570	70.7	75	54	98.9	103	16	28.2
16	41	-1	35000	2874	0.8	612.5	68.9	73.1	72	100.6	103.4	17	31.7
16	43	-1	35000	2983	0.8	655	76	79.4	18	98.7	101.2	17	22.7
16	44	-1	35000	3031	0.8	675	69.5	72.7	54	99	102.1	17	29.5
16	61	-1	35000	2337	0.8	635	67.9	71.3	36	98.8	103.3	17	30.9
17	16	-1	35000	2601	0.8	525	73.8	78.2	36	97.5	101.1	17	23.7
17	41	-1	35000	3094	0.8	710	69.2	73.3	36	98.6	102.7	17	29.4
17	54	-1	40000	2031	0.8	527.5	79.4	82.9	18	95.1	97.9	16	15.7
17	55	-1	40000	2194	0.8	592.5	63.5	65.8	18	98.3	102.4	16	34.8
17	56	-1	40000	2358	0.8	677.5	65.9	68.8	18	92.7	95.7	16	26.8
17	57	-1	40000	2407	0.8	710	69.8	73	36	98.3	102.2	16	28.5
18	9	-1	5000	5017	0.28	527.5	79.4	89	108	83.4	85.3	13	4
18	12	-1	5000	5219	0.28	572.5	81.8	90.7	72	84.8	87	12	3
18	14	-1	5000	5370	0.28	612.5	70	73.1	36	82.4	85.1	13	12.4
18	15	-1	5000	5441	0.28	632.5	70.4	73.2	18	83	85.5	12	12.6

**TABLE 8. PTA IN-FLIGHT STRUCTURE-BORNE NOISE ESTIMATES,
THIRD BLADE PASSAGE TONE - (Continued)**

FLT NO.	RUN NO.	NACL TILT	ALT FT	POWER PSHP	MACH NO.	BPF Hz	STRUCTURE-BORNE			IN-FLIGHT			DELTA
							P3	+SIG	N	P3	+SIG	N	P3
18	16	-1	5000	5503	0.28	655	72.9	75.8	36	79.9	82.3	9	7
18	24	-1	5000	5915	0.42	677.5	76.8	79.7	18	83.4	85.6	16	6.6
19	13	-1	15000	4473	0.35	677.5	71.4	74.4	17	85.7	87.9	17	14.3
19	37	-1	15000	3847	0.5	677.5	77.7	81.6	54	92.5	96	17	14.8
19	44	-1	15000	5110	0.6	677.5	78.7	82	72	104.6	109.4	17	25.9
19	50	-1	15000	5303	0.66	677.5	74.1	76.9	18	110.3	113.7	17	36.2
21	13	-1	15000	5303	0.66	677.5	77.1	79.5	36	109.2	112.9	17	32.1
22	45	-1	27000	3595	0.63	675	69.2	73.2	54	109.9	113.7	17	40.7
22	50	-1	27000	3125	0.47	677.5	73.7	76.8	18	91.9	95.1	16	18.2
23	8	-1	27000	3914	0.73	675	70.2	73.4	18	108.1	111.8	17	37.9
23	11	-1	27000	3970	0.83	592.5	75.1	79.1	54	105.9	110.1	17	30.8
23	17	-1	27000	4312	0.83	705	73.3	76.2	36	99.9	103.4	17	26.6
23	19	-1	27000	3625	0.8	522.5	69.7	73	36	95.4	97.9	17	25.7
23	21	-1	27000	4135	0.8	675	75.6	78.2	54	103.4	108.1	17	27.8
24	28	-1	35000	2773	0.85	520	71.5	75.1	36	98.1	101.5	16	26.6
24	29	-1	35000	2989	0.85	592.5	78.5	82.5	36	102	106	17	23.5
24	33	-1	35000	3202	0.85	675	70.8	74.4	72	97.9	102.1	17	27.1

MAXIMUM
MINIMUM
AVERAGE
STD. DEV.

81.8
63.5
73.3
4.37

90.7
65.8
77.12

112.2
79.9
97.30
8.27

116.2
82.3
100.6

44.6
3
24.00
9.99

AIRCRAFT MODIFICATIONS

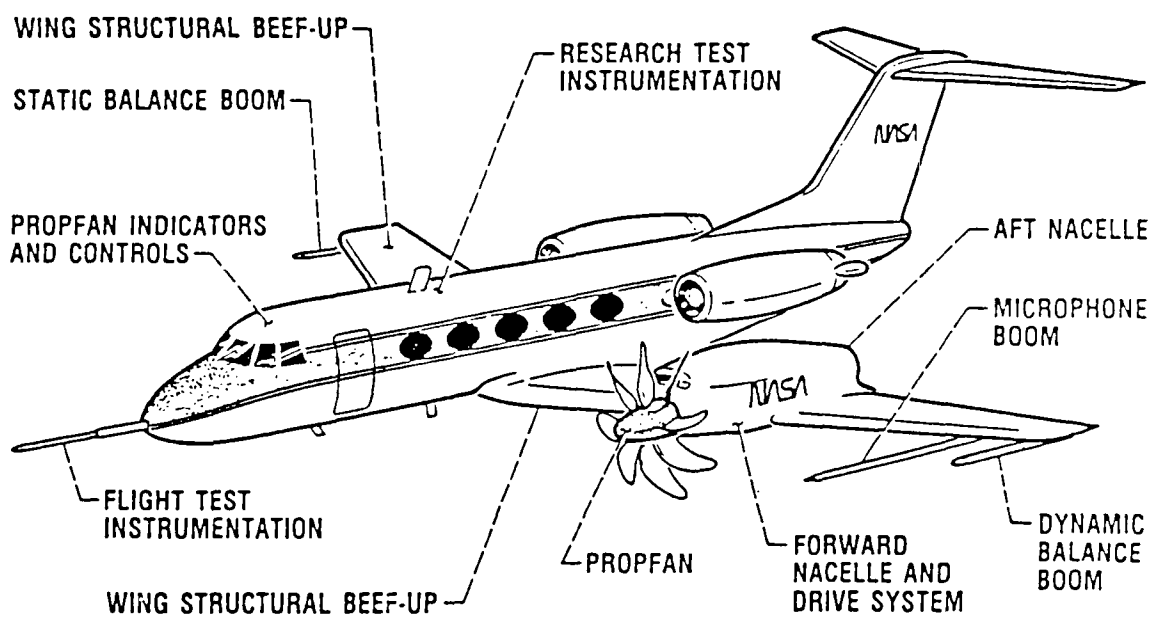


FIGURE 1. PTA TESTBED AIRCRAFT

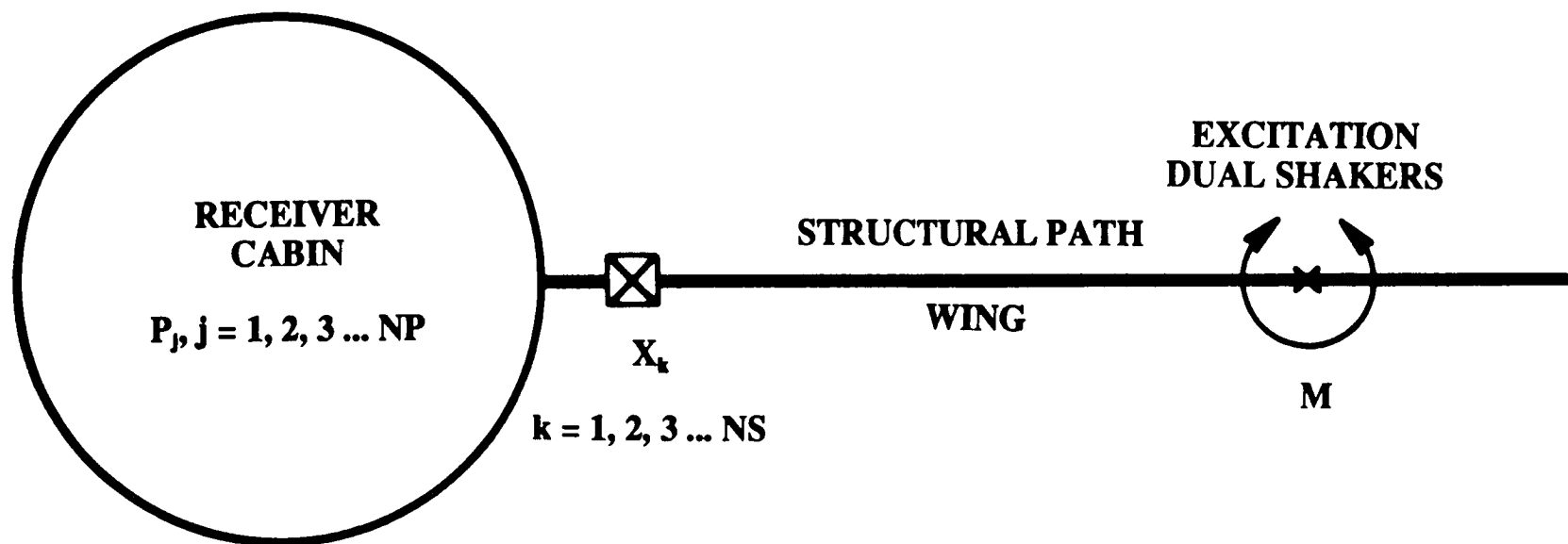


FIGURE 2. IN-FLIGHT STRUCTURE-BORNE NOISE DETECTION CONCEPT

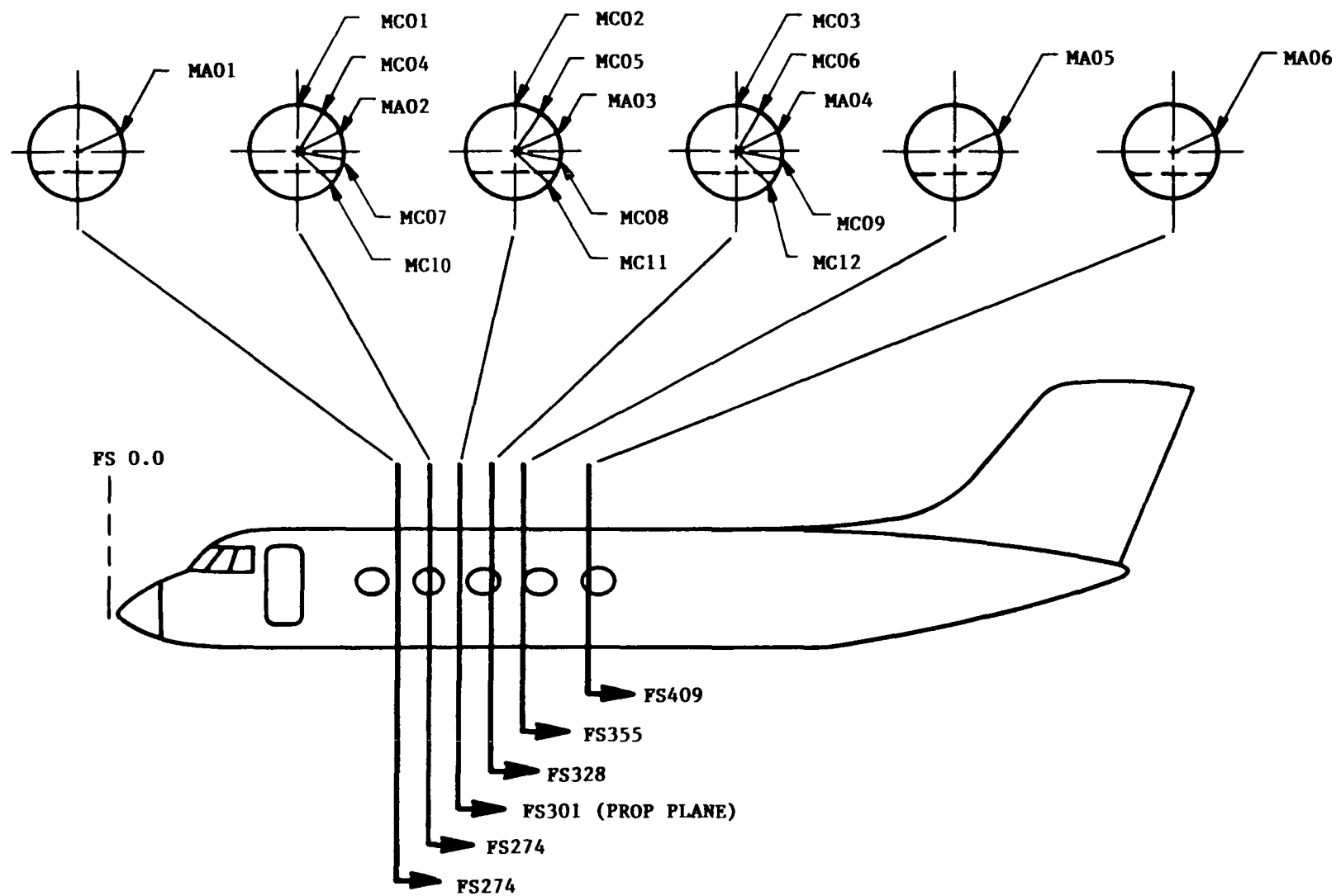


FIGURE 3. CABIN MICROPHONE LOCATIONS

ORIGINAL PAGE
BLACK AND WHITE PHOTOGRAPH

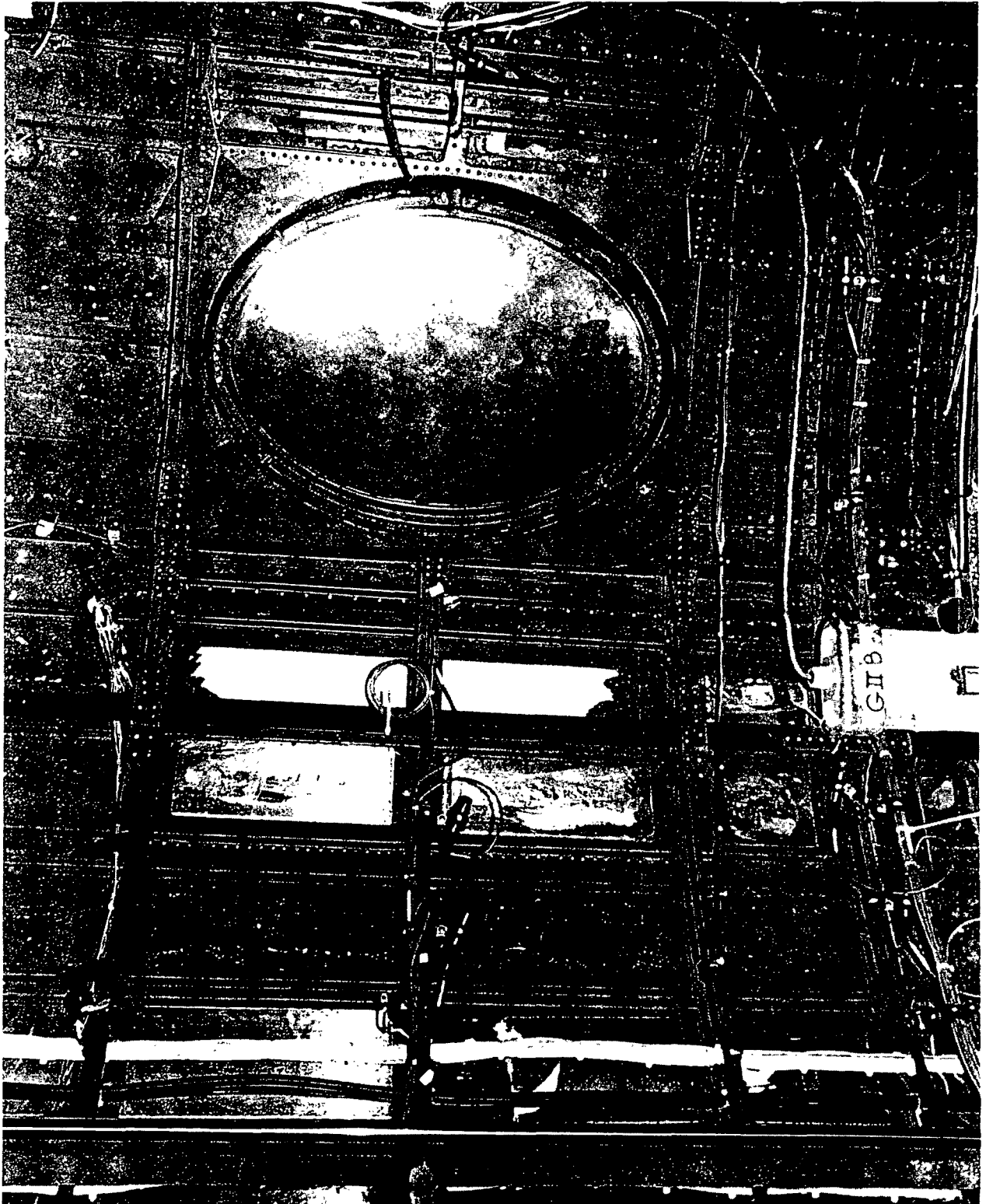


FIGURE 4. TYPICAL IN-FLIGHT FIXED MICROPHONE INSTALLATION

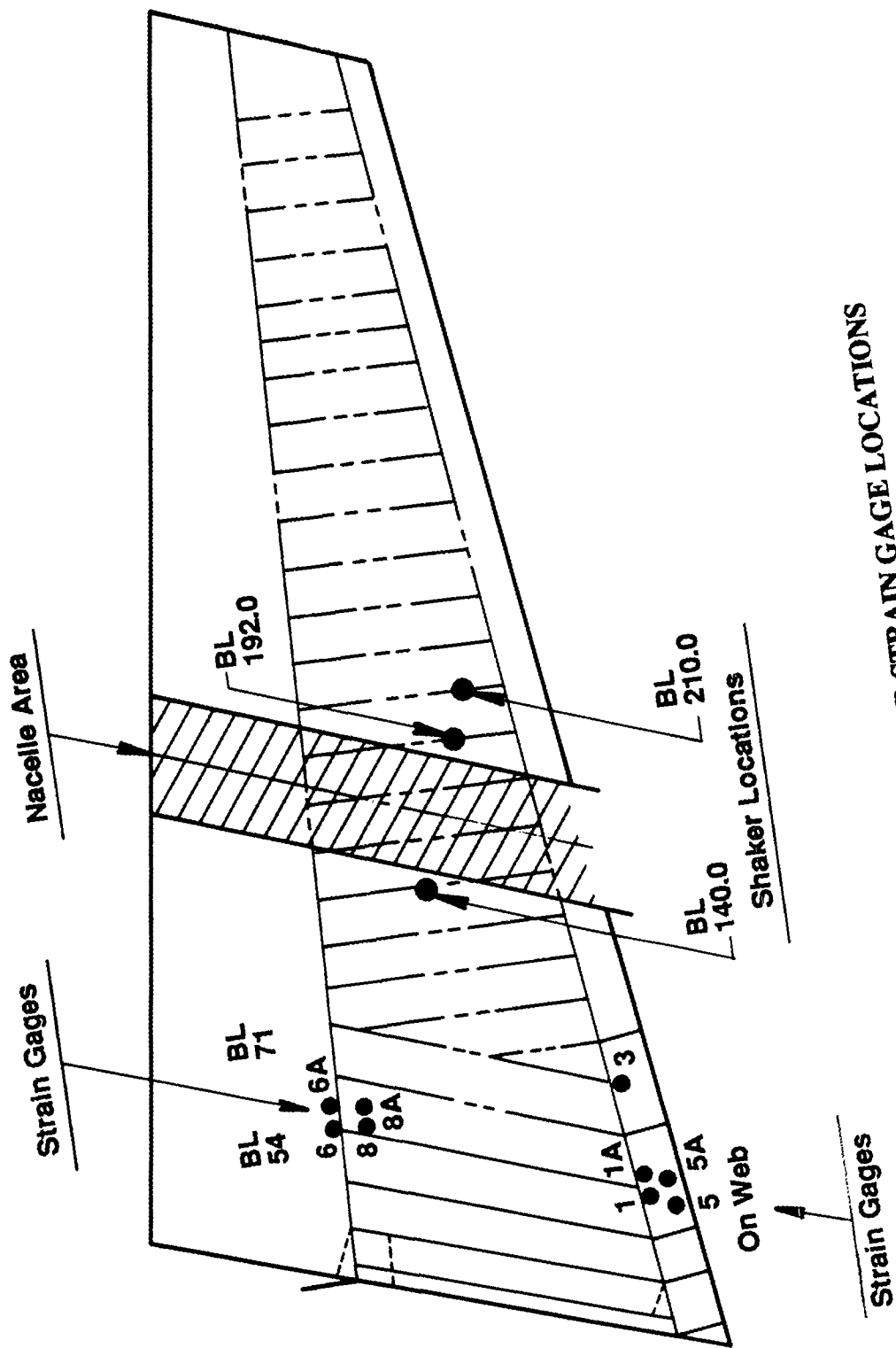
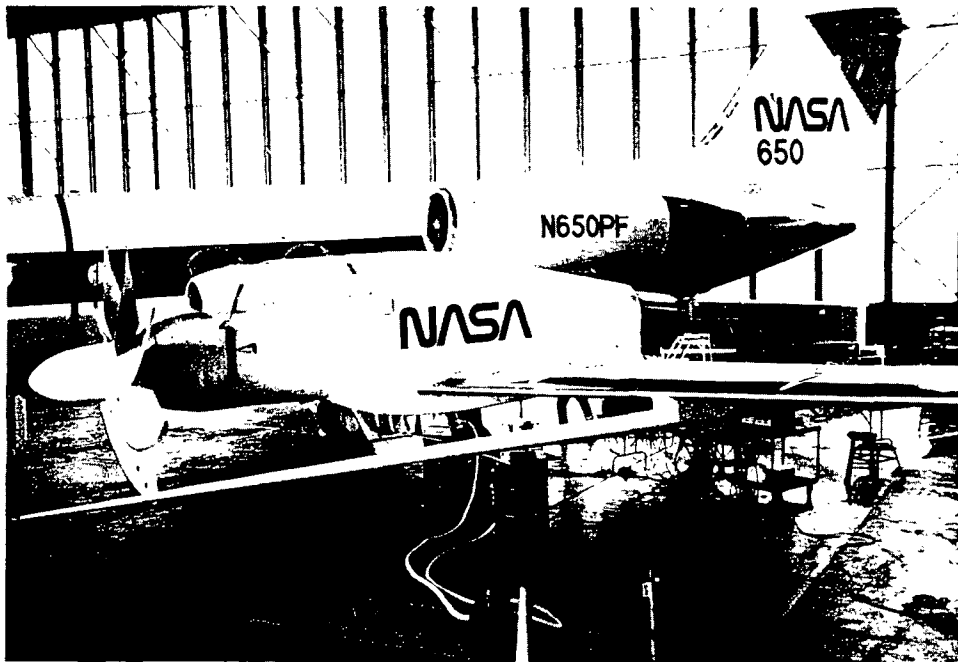


FIGURE 5. SHAKER AND STRAIN GAGE LOCATIONS

ORIGINAL PAGE
BLACK AND WHITE PHOTOGRAPH

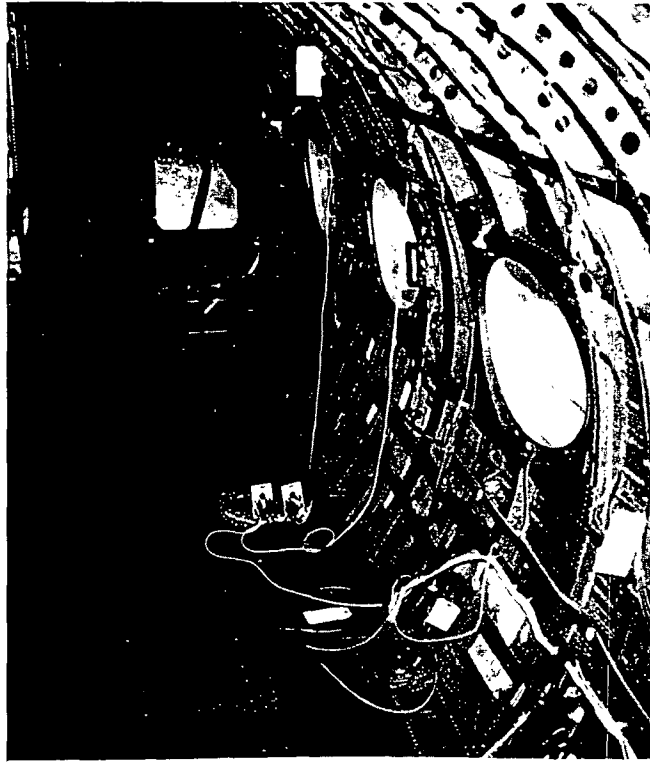


a) General Arrangement of Shaker Installation

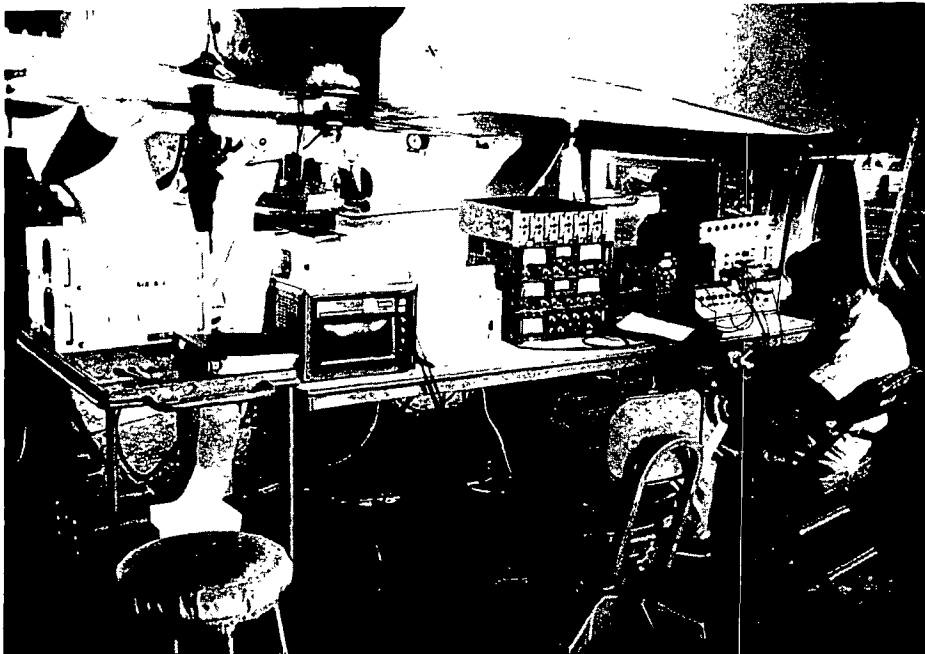


b) Shaker Attachment and Force Cells

FIGURE 6. PHOTOGRAPHS OF TEST SET-UP



c) Typical Microphone Installation



d) General Arrangement of Data Acquisition Equipment

FIGURE 6. PHOTOGRAPHS OF TEST SET-UP (Continued)

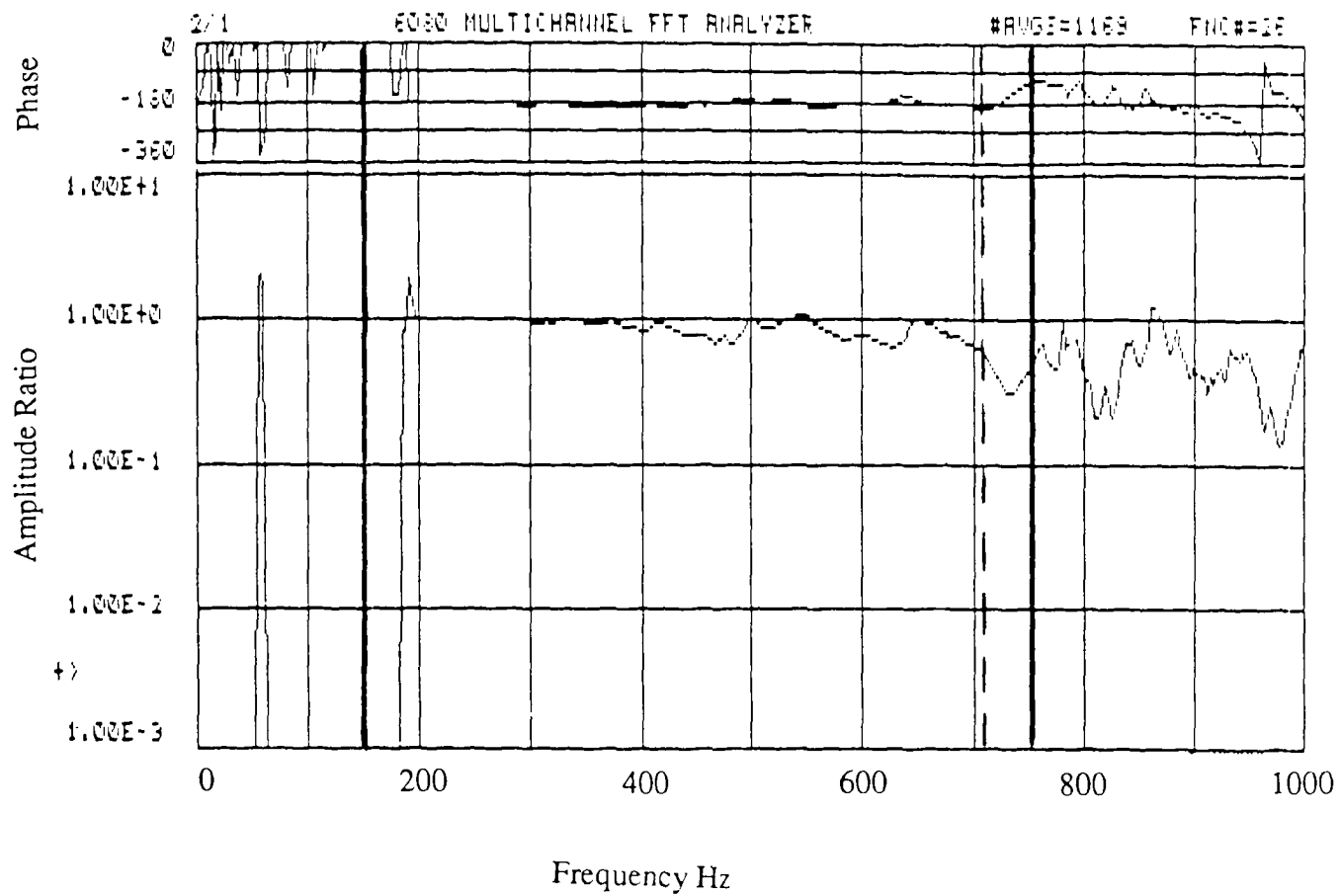


FIGURE 7. FRF RATIO OF SHAKER EXCITATION $F_{\text{INBD}}/F_{\text{OUTBD}}$

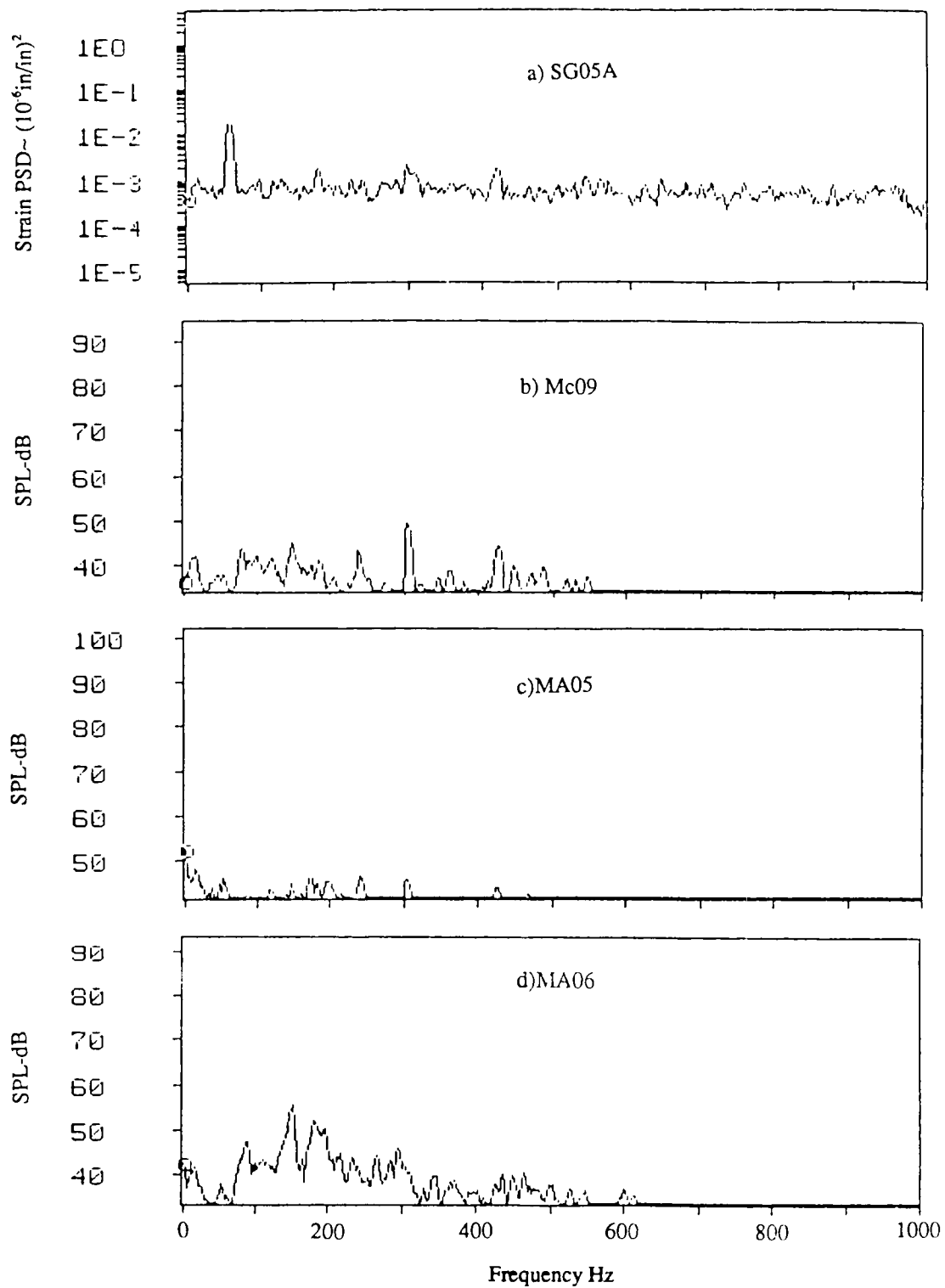


FIGURE 8. TYPICAL BACKGROUND NOISE LEVELS

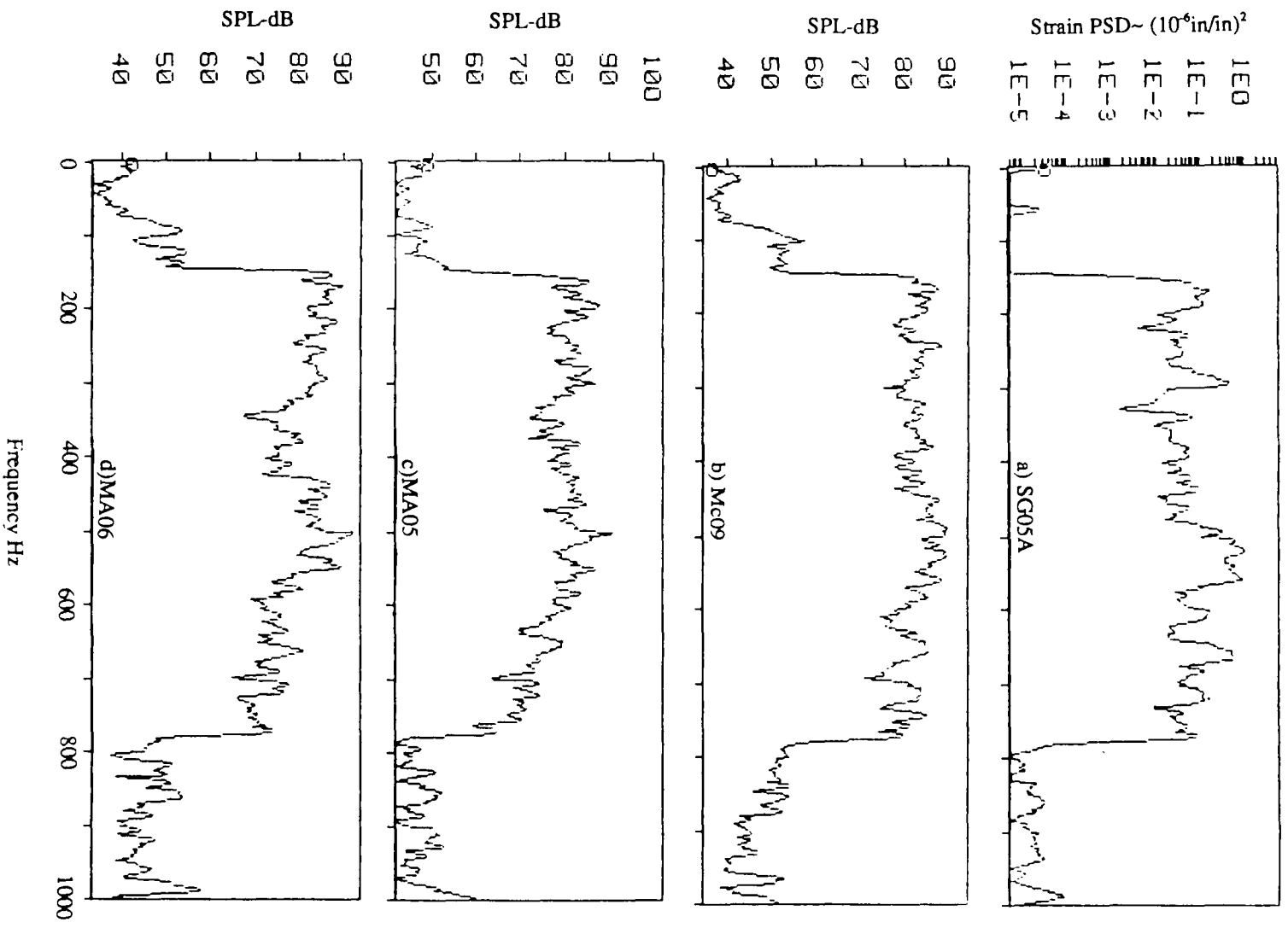


FIGURE 9. TYPICAL RECORDED SIGNAL LEVELS

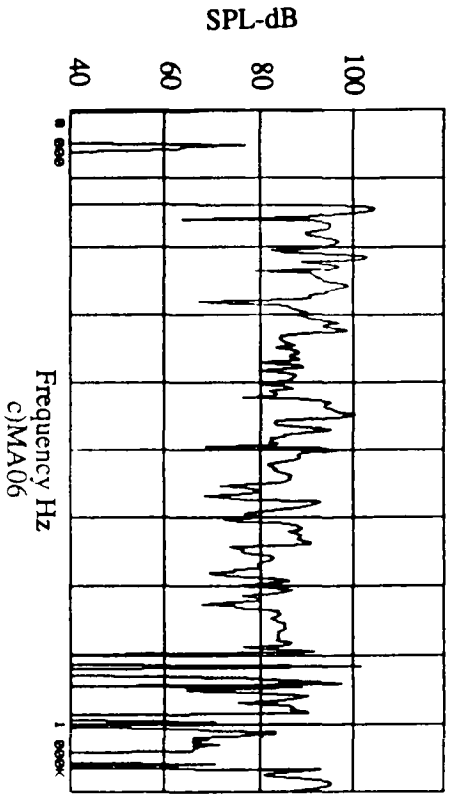
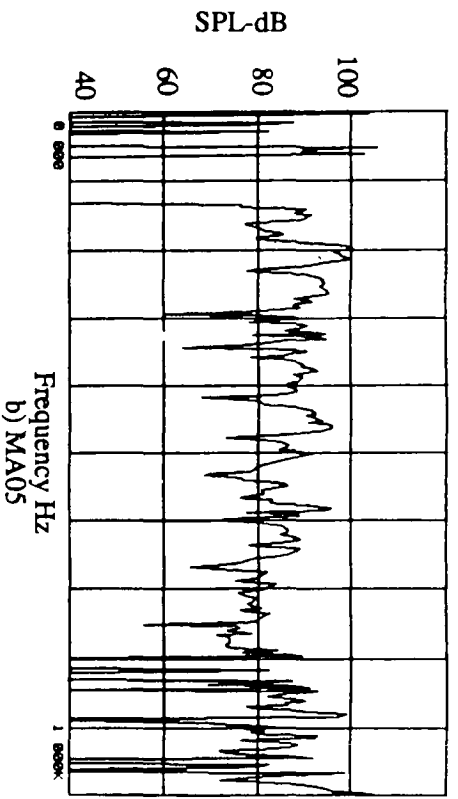
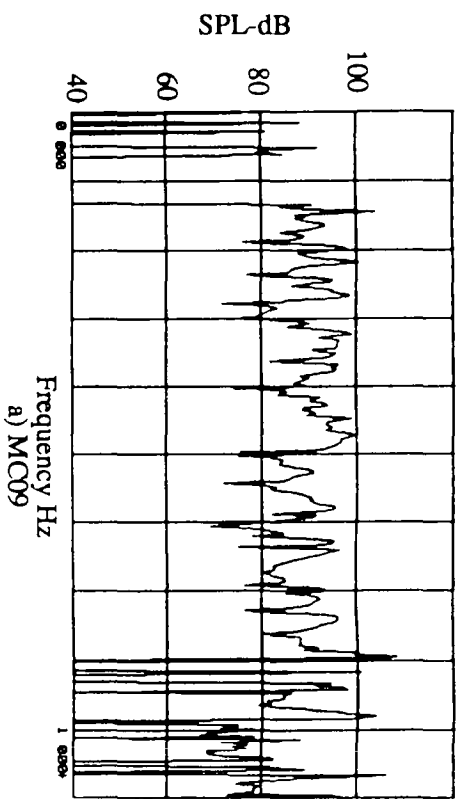


FIGURE 10. INTERIOR SPL RESPONSE TO UNIT MICRO STRAIN AT SG05A

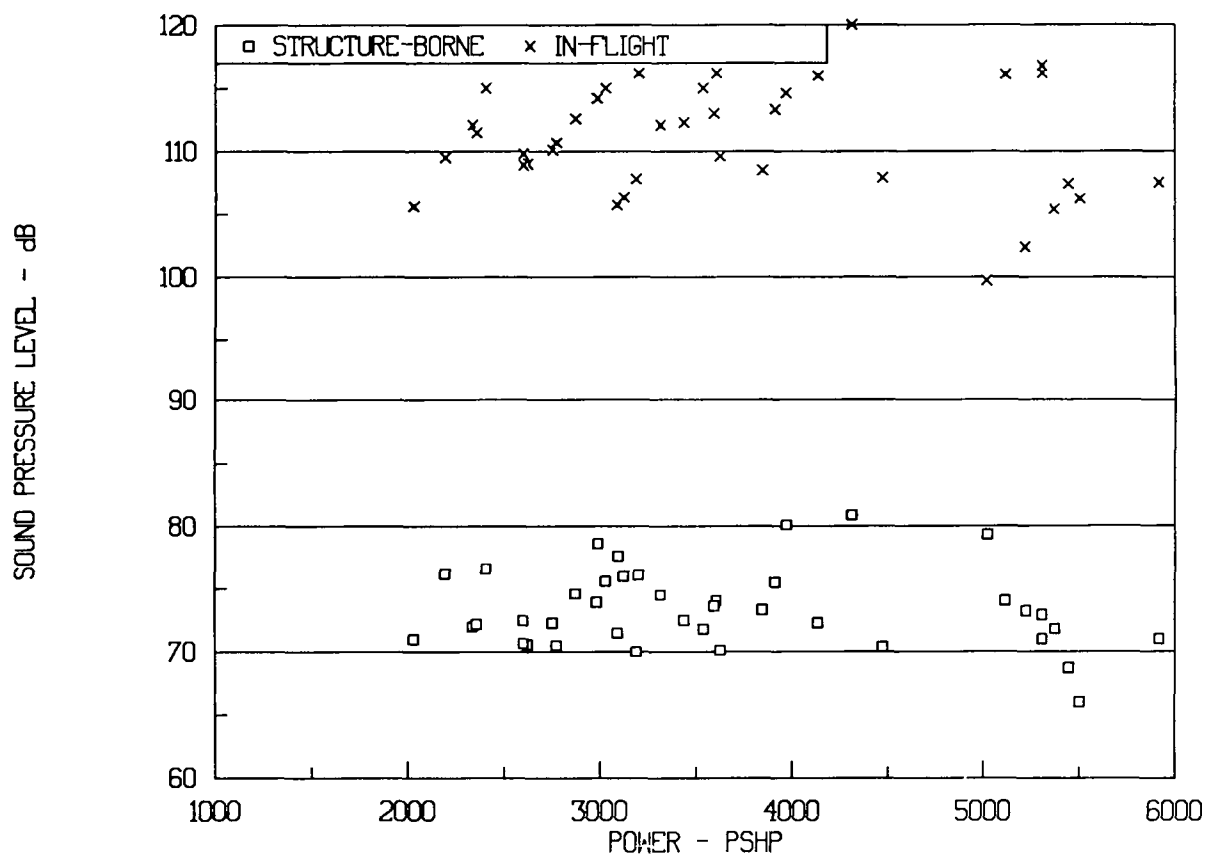


FIGURE 11a. PTA IN-FLIGHT SBN VERSUS ENGINE/PROPELLER POWER, FIRST BLADE PASSAGE TONE

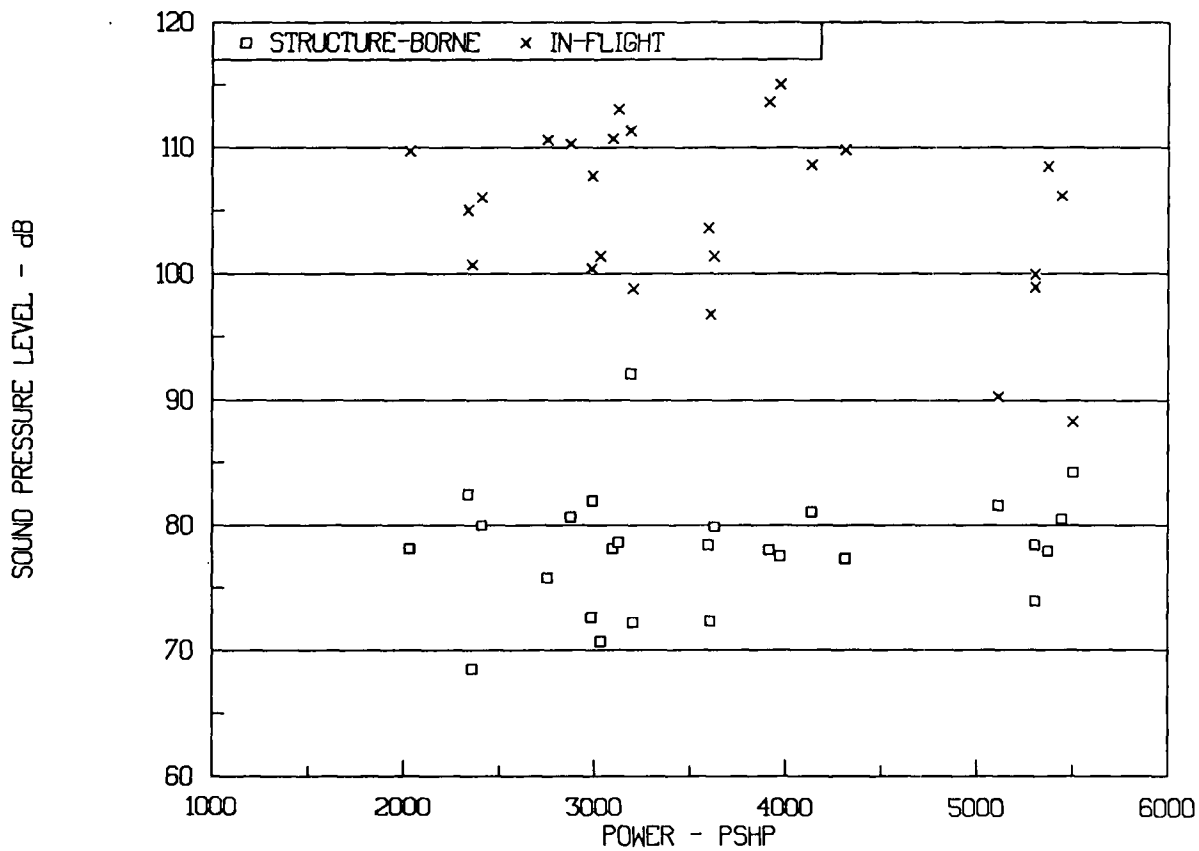


FIGURE 11b. PTA IN-FLIGHT SBN VERSUS ENGINE/PROPELLER POWER,
SECOND BLADE PASSAGE TONE

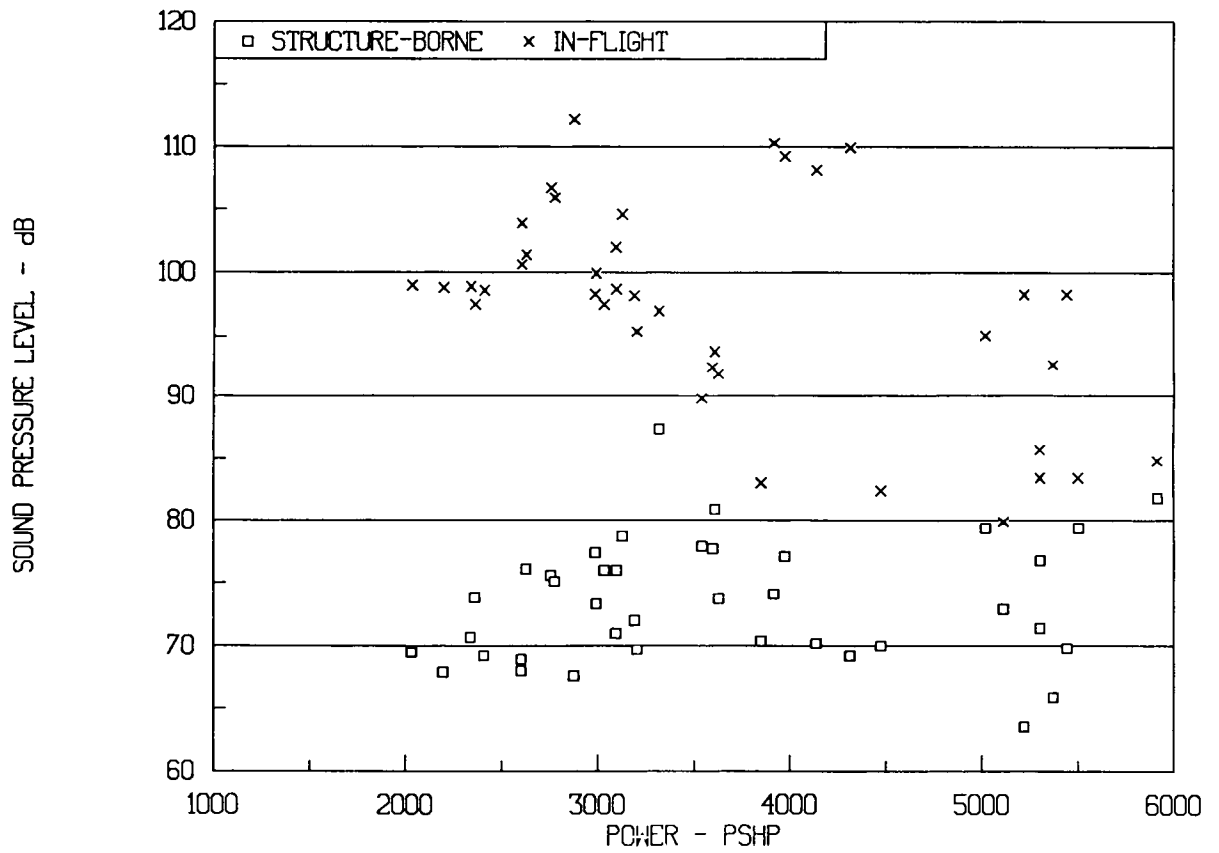


FIGURE 11c. PTA IN-FLIGHT SBN VERSUS ENGINE/PROPELLER POWER, THIRD BLADE PASSAGE TONE

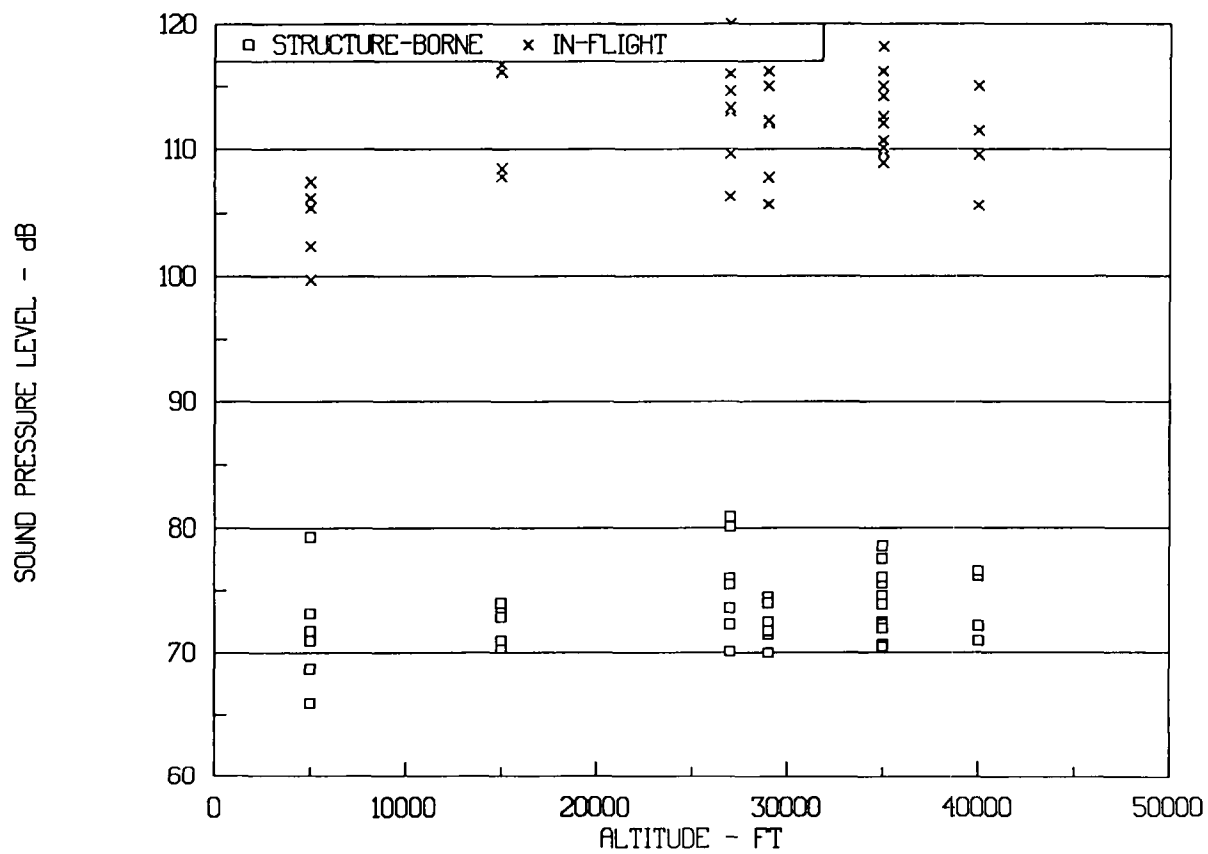


FIGURE 12a. PTA IN-FLIGHT SBN VERSUS FLIGHT ALTITUDE, FIRST BLADE PASSAGE TONE

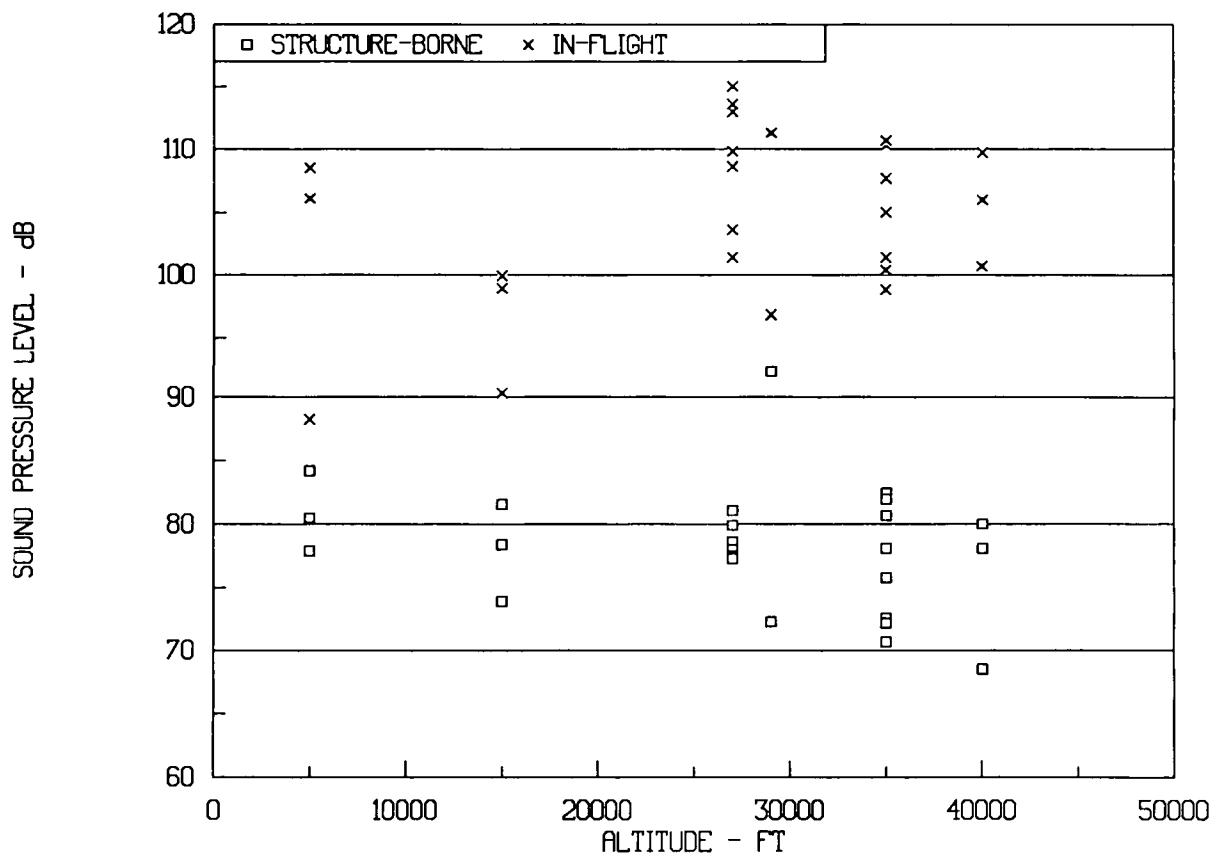


FIGURE 12b. PTA IN-FLIGHT SBN VERSUS FLIGHT ALTITUDE, SECOND BLADE PASSAGE TONE

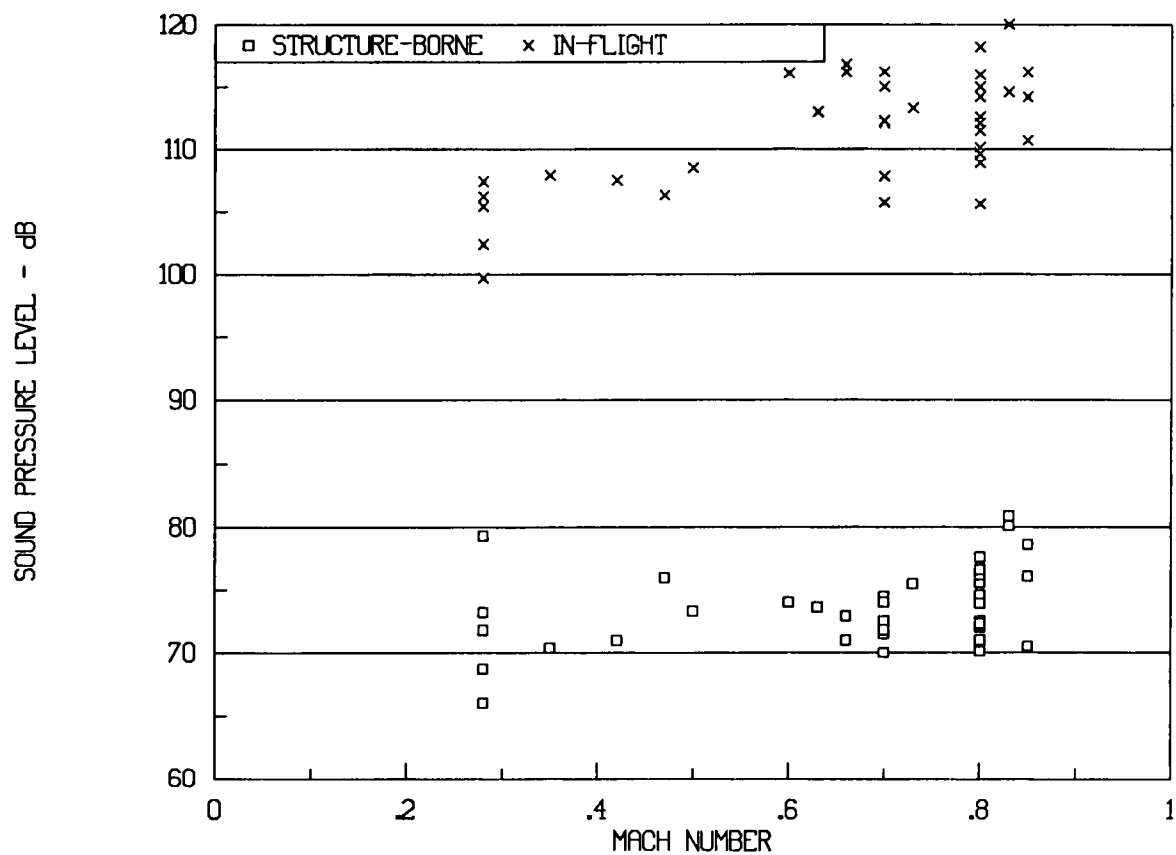


FIGURE 13a. PTA IN-FLIGHT SBN VERSUS MACH NUMBER, FIRST BLADE PASSAGE TONE

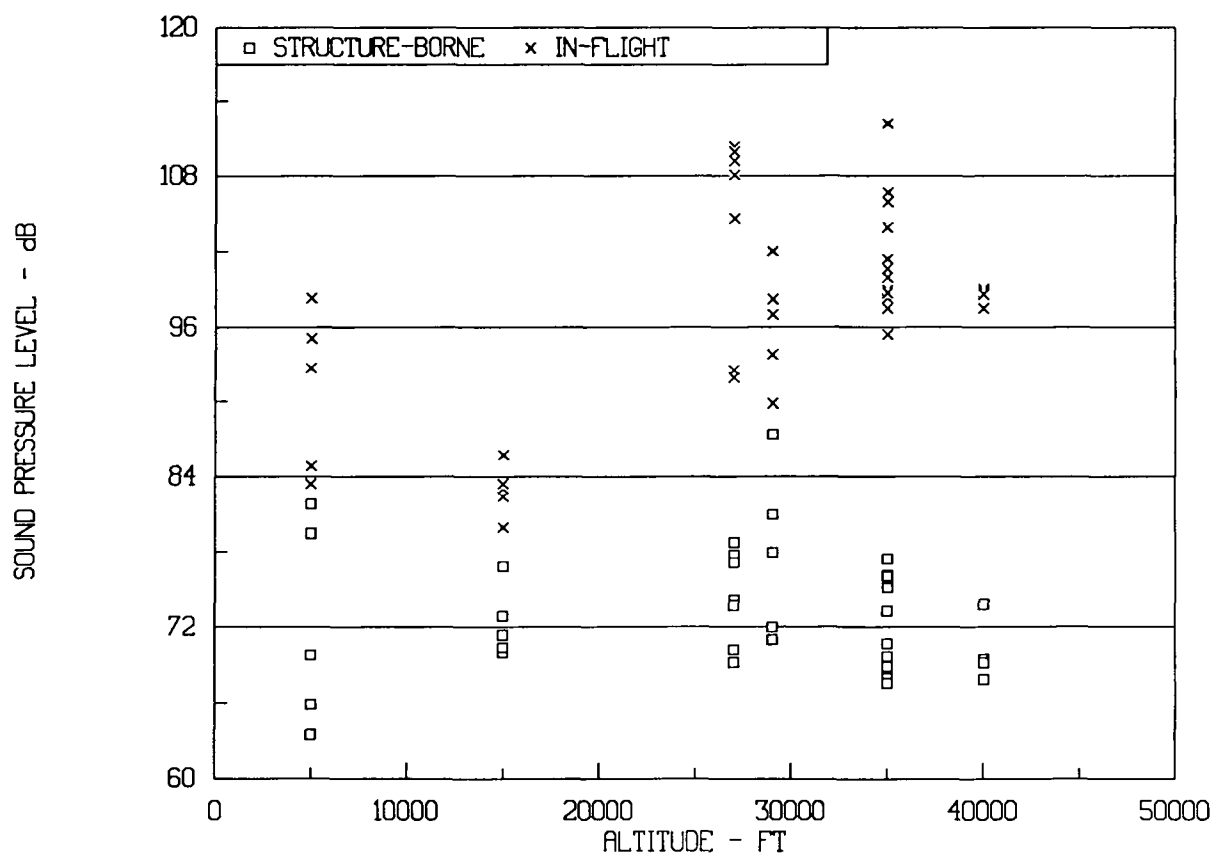


FIGURE 12c. PTA IN-FLIGHT SBN VERSUS FLIGHT ALTITUDE, THIRD BLADE PASSAGE TONE

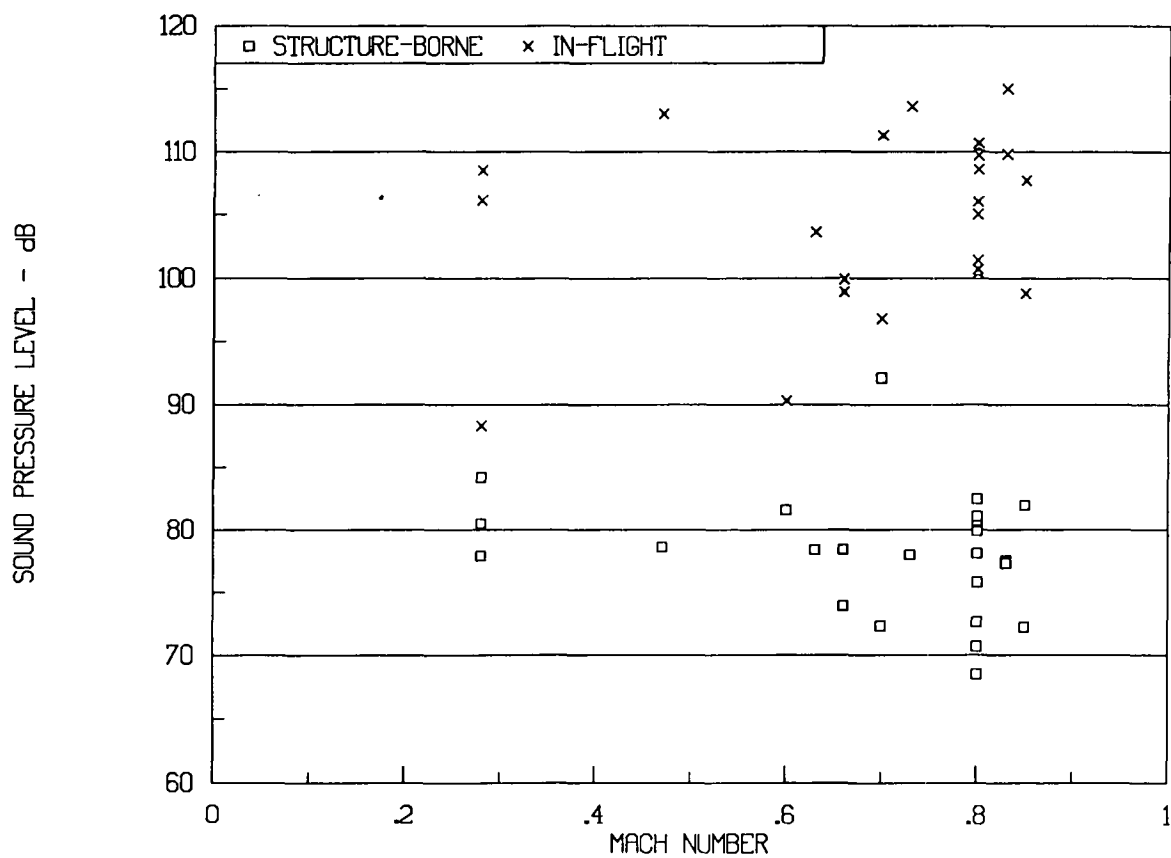


FIGURE 13b. PTA IN-FLIGHT SBN VERSUS MACH NUMBER, SECOND BLADE PASSAGE TONE

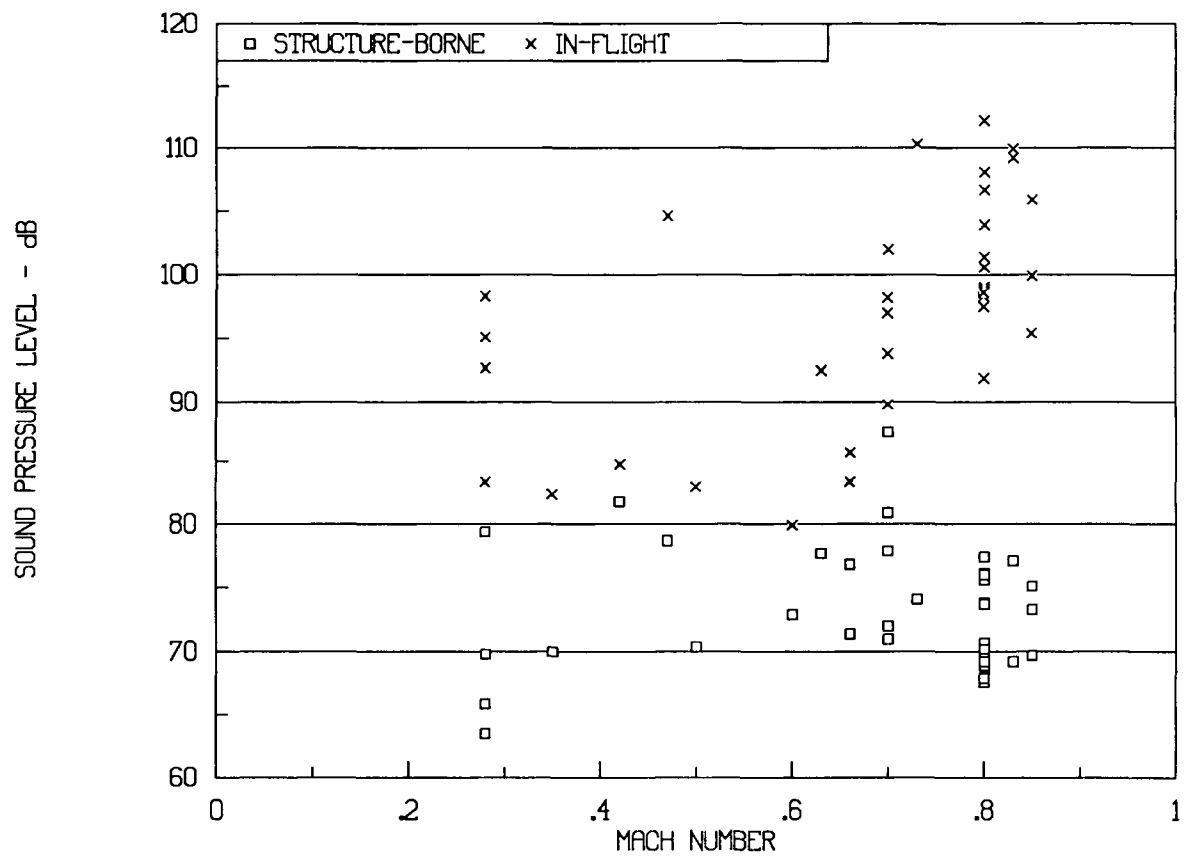


FIGURE 13c. PTA IN-FLIGHT SBN VERSUS MACH NUMBER, THIRD BLADE PASSAGE TONE

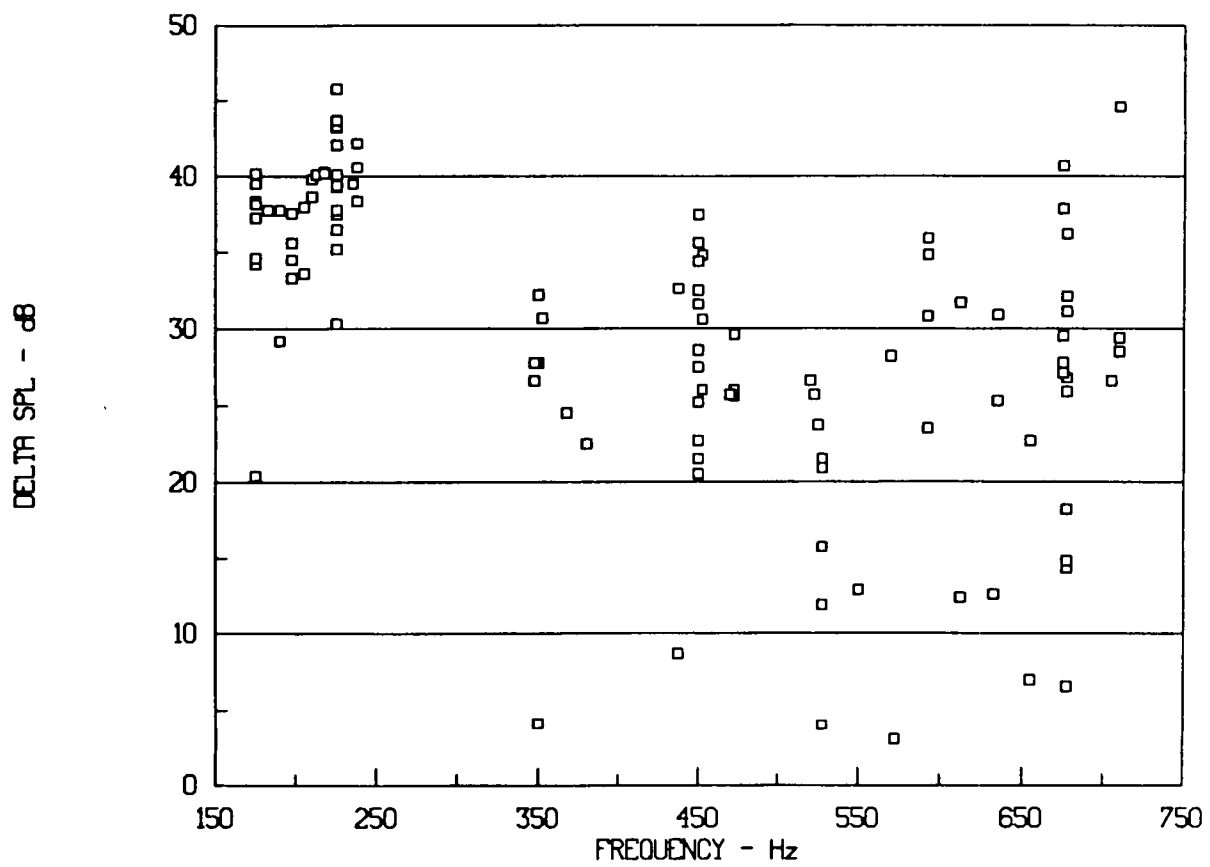


FIGURE 14. DIFFERENCE OF IN-FLIGHT AND STRUCTURE-BORNE NOISE LEVELS VERSUS FREQUENCY



Report Documentation Page

1. Report No. NASA CR-4315	2. Government Accession No.	3. Recipient's Catalog No.	
4. Title and Subtitle Structure-Borne Noise Estimates for the PTA Aircraft		5. Report Date August 1990	
		6. Performing Organization Code	
7. Author(s) James F. Unruh		8. Performing Organization Report No. 04-8542-2	
		10. Work Unit No. 535-03-11-03	
9. Performing Organization Name and Address Southwest Research Institute 6220 Culebra Road, P. O. Box 28510 San Antonio, Texas 78228-0510		11. Contract or Grant No. NAS1-17921	
		13. Type of Report and Period Covered Contractor Report	
12. Sponsoring Agency Name and Address National Aeronautics and Space Administration Langley Research Center Hampton, VA 23665-5225		14. Sponsoring Agency Code	
15. Supplementary Notes Langley Technical Monitors: Kevin Shepherd and Vern L. Metcalf			
16. Abstract Estimates of the level of in-flight structure-borne noise transmission in the Propfan Test Assessment Aircraft were carried out for the first three blade passage frequencies. The procedure used combined the frequency response functions of wing strain to cabin SPL response obtained during ground test with in-flight measured wing strain response data. The estimated cabin average in-flight structure-borne noise levels varied from 64 to 84 dB, with an average level of 74 dB. The estimates showed little dependence on engine/propeller power, flight altitude, or flight Mach number. In general, the bare cabin noise levels decreased with increasing propeller tone giving rise to a plausible structure-borne noise transmission problem at the higher blade passage tones. Without knowledge of the effects of a high insertion loss side wall treatment on structure-borne noise transmission no quantitative conclusions could be made.			
17. Key Words (Suggested by Author(s)) Structure-Borne Noise Aircraft Propellers		18. Distribution Statement Unclassified - Unlimited Subject Category 71	
19. Security Classif. (of this report) Unclassified	20. Security Classif. (of this page) Unclassified	21. No. of pages 68	22. Price A04

National Aeronautics and
Space Administration
Code NTT-4

Washington, D.C.
20546-0001

Official Business
Penalty for Private Use, \$300

BULK RATE
POSTAGE & FEES PAID
NASA
Permit No. G-27



POSTMASTER: If Undeliverable (Section 158
Postal Manual) Do Not Return
